National Cooperative Highway Research Program

NCHRP Report 354

Resistance of Welded Details Under Variable Amplitude Long-Life Fatigue Loading

Transportation Research Board
National Research Council

National Cooperative Highway Research Program

Report 354

Resistance of Welded Details Under Variable Amplitude Long-Life Fatigue Loading

J. W. FISHER, A. NUSSBAUMER, P. B. KEATING,
and B. T. YEN
Center for Advanced Technology for Large Structural Systems
Lehigh University
Bethlehem, Pennsylvania

Research Sponsored by the American Association of State Highway and Transportation Officials in Cooperation with the Federal Highway Administration

TRANSPORTATION RESEARCH BOARD
NATIONAL RESEARCH COUNCIL

NATIONAL ACADEMY PRESS
Washington, D.C. 1993

NATIONAL COOPERATIVE HIGHWAY RESEARCH PROGRAM

Systematic, well-designed research provides the most effective approach to the solution of many problems facing highway administrators and engineers. Often, highway problems are of local interest and can best be studied by highway departments individually or in cooperation with their state universities and others. However, the accelerating growth of highway transportation develops increasingly complex problems of wide interest to highway authorities. These problems are best studied through a coordinated program of cooperative research.

In recognition of these needs, the highway administrators of the American Association of State Highway and Transportation Officials initiated in 1962 an objective national highway research program employing modern scientific techniques. This program is supported on a continuing basis by funds from participating member states of the Association and it receives the full cooperation and support of the Federal Highway Administration, United States Department of Transportation.

The Transportation Research Board of the National Research Council was requested by the Association to administer the research program because of the Board's recognized objectivity and understanding of modern research practices. The Board is uniquely suited for this purpose as: it maintains an extensive committee structure from which authorities on any highway transportation subject may be drawn; it possesses avenues of communications and cooperation with federal, state and local governmental agencies, universities, and industry; its relationship to the National Research Council is an insurance of objectivity; it maintains a full-time research correlation staff of specialists in highway transportation matters to bring the findings of research directly to those who are in a position to use them.

The program is developed on the basis of research needs identified by chief administrators of the highway and transportation departments and by committees of AASHTO. Each year, specific areas of research needs to be included in the program are proposed to the National Research Council and the Board by the American Association of State Highway and Transportation Officials. Research projects to fulfill these needs are defined by the Board, and qualified research agencies are selected from those that have submitted proposals. Administration and surveillance of research contracts are the responsibilities of the National Research Council and the Transportation Research Board.

The needs for highway research are many, and the National Cooperative Highway Research Program can make significant contributions to the solution of highway transportation problems of mutual concern to many responsible groups. The program, however, is intended to complement rather than to substitute for or duplicate other highway research programs.

Note: The Transportation Research Board, the National Research Council, the Federal Highway Administration, the American Association of State Highway and Transportation Officials, and the individual states participating in the National Cooperative Highway Research Program do not endorse products or manufacturers. Trade or manufacturers names appear herein solely because they are considered essential to the object of this report.

NCHRP REPORT 354

Project 12-15(5) FY'82

ISSN 0077-5614

ISBN 0-309-05352-8

L. C. Catalog Card No. 93-060200

Price $10.00

Areas of Interests

Bridges, Other Structures, and Hydraulics and Hydrology
Maintenance

Modes

Highway Transportation
Public Transit
Rail Transportation

NOTICE

Published reports of the

NATIONAL COOPERATIVE HIGHWAY RESEARCH PROGRAM

are available from:

Transportation Research Board
National Research Council
2101 Constitution Avenue, N.W.
Washington, D.C. 20418

Printed in the United States of America

FOREWORD

By Staff
Transportation Research Board

This report contains the results of a study that extended the findings contained in *NCHRP Report 267,* "Steel Bridge Members Under Variable Amplitude Long Life Fatigue Loading," by providing additional information on fatigue crack growth behavior of steel bridge members under randomly applied, variable amplitude loadings in the extreme life region. The findings of this study will be of interest to engineers, researchers, members of specification writing bodies, and others concerned with the design, construction, and maintenance of steel structures.

Fatigue cracks have developed at the ends of cover plates in beams that are only infrequently subjected to stress ranges exceeding the fatigue limit of AASHTO's Category E′. Small cracks have been detected in beams where only 0.1 percent of the measured stress cycles exceeded the estimated fatigue limit. This observed field behavior suggests that more severe fatigue problems could result if bridges are subjected to heavier loads in the future. Futhermore, the consequences of occasional overloads from permits and other sources may be more critical than previously believed.

Significant reductions in fatigue life of many welded details occur when cracks initiate and grow from micro-sized defects that exist at the weld periphery. This behavior has been demonstrated by studies on cover-plated beams and other structural details, and has been reported in *NCHRP Report 102,* "Effect of Weldments on the Fatigue Strength of Steel Beams"; *NCHRP Report 147,* "Fatigue Strength of Steel Beams with Welded Stiffeners and Attachments"; *NCHRP Report 188,* "Welded Steel Bridge Members Under Variable-Cycle Fatigue Loadings"; *NCHRP Report 206,* "Detection and Repair of Fatigue Damage in Welded Highway Bridges"; *NCHRP Report 227,* "Fatigue Behavior of Full-Scale Welded Bridge Attachments"; and *NCHRP Report 267,* "Steel Bridge Members Under Variable Amplitude Long Life Fatigue Loading."

This report contains the findings of NCHRP Project 12-15(5), "Fatigue Behavior of Variable Loaded Bridge Details Near the Fatigue Limit." The previously available test data on long-life fatigue behavior were very sparse and did not provide an adequate basis on which to assess the problem. NCHRP Project 12-15(5) provided additional information on fatigue crack growth behavior by subjecting eight full-sized welded girders incorporating three types of welded details—partial length cover plates, web attachments, and transverse web stiffeners—to long-life, variable amplitude loading. Welded details simulating attachments used on bridge members were subjected to variable amplitude loading similar to the skewed spectra that most bridge structures experience. The results obtained from these variable amplitude tests supplemented and further verified the observations reported in *Report 267.* The findings support the conservative design assumption that a straight line extension of the fatigue-resistance curves for Category E and E′ details, largely developed from constant amplitude loading, can be used to predict the fatigue life of details subjected to variable life loading. The straight line extension appears to be overly conservative for higher strength details such as transverse stiffeners.

CONTENTS

RESISTANCE OF WELDED DETAILS UNDER VARIABLE AMPLITUDE LONG-LIFE FATIGUE LOADING

SUMMARY

The research described in this report is the result of continued experimental studies performed in the laboratory under NCHRP Project 12-15(5). It is intended to provide additional information on the effects of infrequently exceeding the constant amplitude fatigue limit during the service life of bridge structures. Welded details simulating attachments used on steel bridge members were subjected to variable amplitude loading similar to the skewed spectra that most bridge structures experience. Only a few stress cycles exceeded the constant amplitude fatigue limit for a number of the welded details that were tested.

Eight full-size welded girders with Category E′ web attachments and cover-plated flanges and Category C transverse stiffeners and diaphragm connection plates were tested during the program. The welded girders were primarily subjected to in-plane loading. A few diaphragm connection plate details were simultaneously subjected to out-of-plane deformation as well.

The results obtained from the variable amplitude tests were found to supplement and further verify the observations reported in *NCHRP Report 267*. The test results, using Category E′ welded web attachments, demonstrated that the lower bound fatigue life was reasonably well represented by extension of the exponential relationship even when the effective stress range for the detail was below the constant amplitude fatigue limit. Under long-life loading, cumulative frequencies of cycles, which exceeded the constant amplitude fatigue limit by more than 0.05 percent, resulted in fatigue cracking. Similar results were obtained from tests of Category E′ cover plate details without transverse end welds. For these details, when the effective stress range was below the constant amplitude fatigue limit, cumulative exceedance frequencies greater than 4.3 percent resulted in fatigue cracks. The results on the Category E′ cover plate details were compatible with the results in *NCHRP Report 267* on Category E cover plate details ($t_f < 0.8$ in.).

Truncating the smaller stress cycles in the final pair of test girders resulted in fatigue cracking at higher levels of effective stress range. The test results remained compatible with the full spectrum tests and fell above the lower bound Category E′ fatigue-resistance curve.

The tests on stiffener details classified as Category C details only resulted in four cracks in 20 details. Two of these details developed cracks during the 120 million variable stress cycles, although only 11,000 cycles (0.01 percent) of the variable cycles exceeded the constant amplitude fatigue limit. The test data all plotted well beyond the extension of the Category C fatigue resistance curve. In addition, the peak stress cycle was at or above 16 ksi.The test results on the stiffener details suggest that these details are not likely to

develop fatigue cracks in service. Available field test data on bridges indicate that the constant amplitude fatigue limit will not likely be exceeded often enough to cause significant damage.

The study also demonstrated that large web gap stresses from distortion were as serious under variable amplitude loading as under constant cycle loading. The test results were comparable to those reported in *NCHRP Report 336.*

CHAPTER 1

INTRODUCTION AND RESEARCH APPROACH

Fatigue cracks have developed at the ends of cover plates in beams that are only infrequently subjected to stress ranges exceeding the fatigue limit of AASHTO's Category E′ (*1*). For example, in one particular structure, small cracks have been detected in several beams where only 0.1 percent of the measured stress cycles exceeded the estimated fatigue limit. This observed field behavior suggests that more severe fatigue problems could result if bridges are subjected to heavier loads in the future, and the consequences of occasional overloads from permits and other sources may be more critical than previously assumed.

The consequence of initiating fatigue crack growth in existing bridges as a result of increased loads could have major impact on the life expectancy and the safety of bridges on high-volume arteries where large numbers of random variable stress cycles are expected. The available test data in the high-cycle region of behavior are sparse and do not provide an adequate basis on which to assess this problem.

Fatigue test results from several prior studies indicated that fatigue cracks develop in test specimens even though the effective stress range is well below the crack growth threshold or fatigue limit (*2–4*). Stress cycles below the fatigue limit do not result in fatigue crack propagation when all variable stress cycles or constant amplitude stress cycles are under the fatigue limit. When all variable load cycles or constant amplitude loadings are below the constant amplitude fatigue limit (CAFL), no fatigue crack propagation occurs. The constant amplitude fatigue limit is typically shown as a horizontal extension of the S-N fatigue design curve for a given detail. The types of specimens tested varied from small-scale attachment details to full-scale cover-plated beams. The percentage of cycles exceeding the constant amplitude fatigue limit for these tests ranged from 100 percent to as few as 0.24 percent. However, the studies in References *3* and *4* were limited in scope in that only a few detail types were tested, and with those, a limited number of tests were run. This approach resulted in little or no replication of data.

The NCHRP Project 12-15(4) test program (*2*) was initiated in 1979 with the objective to expand the existing database through the use of full-scale beams. Eight rolled W18X50 beams of A588 steel with a span length of 15 ft (4.6 m) were used. Two types of welded attachments were incorporated: 1-in. × 4½-in. (25.4 mm × 114 mm) partial length cover plates (Category E details) and 1.0-in. (25.4-mm) thick by 12.0-in. (305-mm) long fillet-welded web attachments (Category E′ details). All beams were tested in their as-fabricated state. The Category E and E′ welded details produced local residual tensile stresses near enough to the yield stress of the material so that variations of the R-ratio, $\sigma_{min}/\sigma_{max}$, downward from unity were relatively small and could be disregarded. A Rayleigh-type skewed distribution was used for the stress range spectrum. Fatigue limit exceedance rates, held constant for a given test, varied from 0.10 to 11.72 percent for the program.

The test results from Project 12-15(4) indicated that all stress cycles in the spectrum contributed to fatigue damage and fatigue crack propagation. The calculated effective stress range using the Root Mean Cube (RMC) based on Miner's Rule was observed to provide a lower bound fatigue resistance even though the calculated effective stress range was below the constant amplitude fatigue limit. The results were found to be independent of the exceedance rate for the Category E and E′ details examined in the study. This suggested that all stress cycles would need to be below the fatigue limit for no fatigue crack growth.

OBJECTIVES AND SCOPE

The objective of this study was to extend the findings of Project 12-15(4) by providing additional information on fatigue crack growth behavior of steel bridge members under randomly applied, variable amplitude loadings in the fatigue limit, extreme life region. Testing was carried out on eight full-scale welded girders, which incorporated three types of welded details: (1) partial length cover plates, (2) web attachments, and (3) transverse web stiffeners. The partial length cover plates and web attachment details both provided a Category E′ fatigue classification as a result of the detail geometry and flange thickness. The transverse stiffeners were all cut short of the tension flange and provided a Category C fatigue detail.

The currently available test data pertaining to rarely occurring high loads above the constant cycle fatigue limit are very sparse and do not provide an adequate basis on which to assess this problem. The consequences of triggering fatigue crack growth in existing bridges as a result of increased loads could have a major impact on the life expectancy and safety of bridges on high-volume arteries where large numbers of random variable stress cycles are expected.

In addition to the test program directed at the primary objective, a small portion of the total effort was expended on a reassessment of the fatigue specifications in the AASHTO *Standard Specifications for Highway Bridges.* Minor revisions to the fatigue design provisions were recommended to, and adopted by, the AASHTO Subcommittee on Bridges and Structures in 1988. The test evaluation and the recommended specifications were published in *NCHRP Report 286,* "Evaluation of Fatigue Test Data and Design Criteria on Welded Details," in September 1986 (*5*).

RESEARCH APPROACH

Laboratory Tests of Full-Scale Girders

NCHRP Project 12-15(5) involved the fatigue testing of eight full-scale welded plate girders. All web, flange plates and attach-

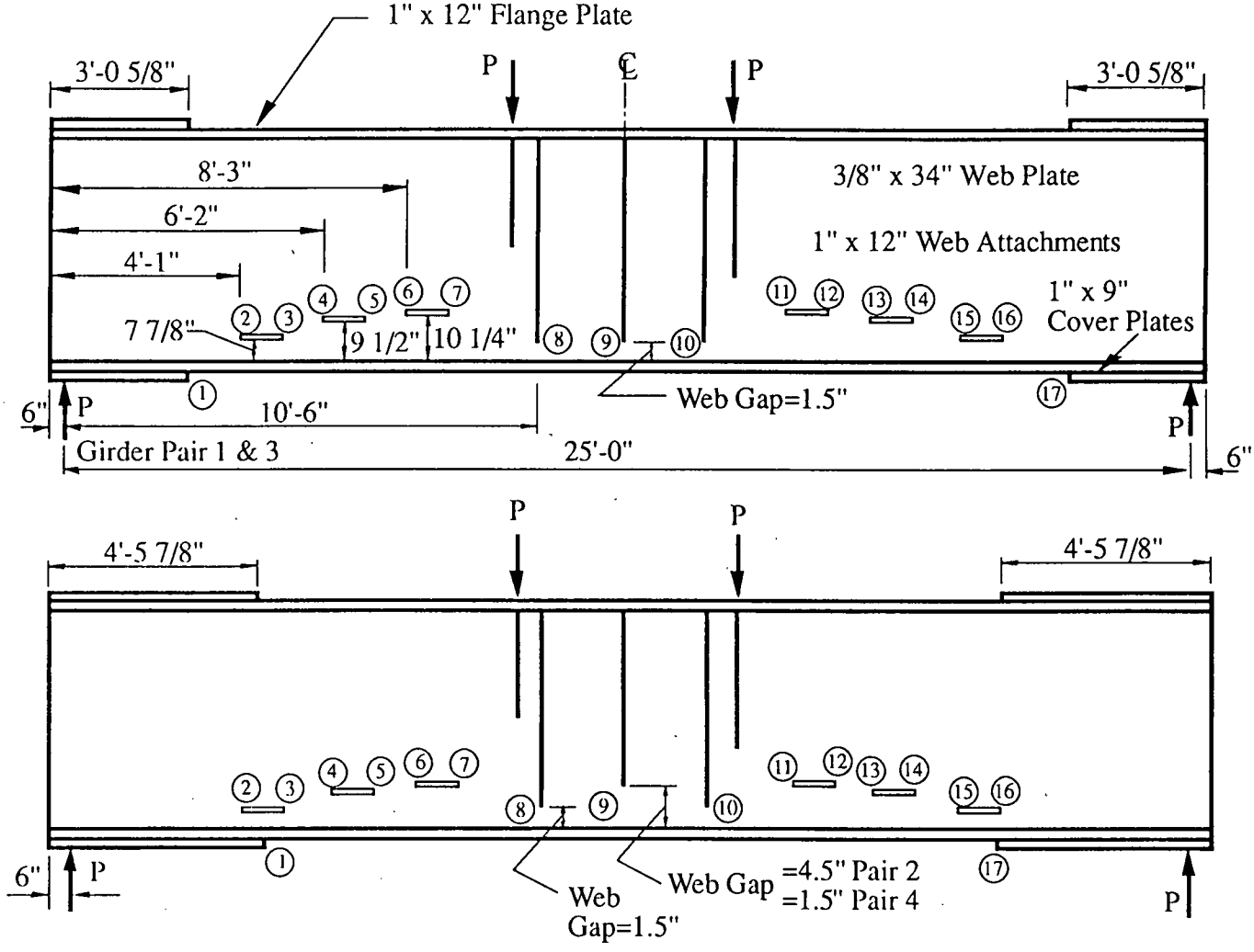

Figure 1. Schematic of girder pairs.

ments were A36 steel. Tensile tests of the $\frac{3}{8}$-in. (9.5-mm) web plate showed an average yield level of 45.3 ksi (312 MPa) and a tensile strength of 68.6 ksi (473 MPa). The 1-in. (254-mm) thick flanges, web attachments, and cover plates had an average yield level of 38.6 ksi (266 MPa) and a tensile strength of 68.9 ksi (475 MPa). Each girder was 26 ft (8 m) long, and they were tested in identical pairs on a 25-ft (7.6-m) span under four-point loading. Schematics of the test girders are shown in Figure 1. The girders were 36 in. (914 mm) deep with 1- × 12-in. (25- × 305-mm) flanges and a $\frac{3}{8}$-in. (9.5-mm) thick web plate. Three detail types were fillet-welded to the girders: partial length cover plates, web attachments, and transverse web stiffeners. The cover plates were 1- × 9-in. (25- × 228-mm) plates, either with or without transverse end welds. Girder Pair 1 had transverse end welds and the shortest length cover plates. Girder Pair 3 had cover plates with and without end welds and short length cover plates. Girder Pairs 2 and 4 had cover plates with no end welds, which overlapped by 5 in. (127 mm) the web attachments nearest the end supports. The cover plate details provide a Category E′ classification because the flange thickness is greater than 0.8 in. (20 mm). The web attachments all consist of 1.0-in. (25-mm) thick by 12-in. (305-mm) long plates with longitudinal fillet welds only. These are also Category E′ details due to their thickness and length. As can be seen in Figure 1, all six web attachments were located in the same positions on all eight test girders. The $\frac{3}{8}$- × 3.0-in. (9.5- × 76-mm) transverse web stiffeners (Category C) were cut short of the tension flange with a $1\frac{1}{2}$-in. (38-mm) web gap on Girder Pairs 1, 3, and 4. Each test girder has 17 possible fatigue crack locations.

In addition to the three detail types used to study in-plane fatigue behavior, each plate girder contained a diaphragm connection plate detail at midspan. The connection plate was cut short of the tension flange by either $1\frac{1}{2}$ in. (38 mm) or $4\frac{1}{2}$ in. (114 mm) on Girder Pair 2 in order to provide an unstiffened web gap that could be subjected to out-of-plane distortion under variable amplitude load conditions.

A wide-band Rayleigh-type stress range spectrum was used. The variable amplitude stress spectrum for Girder Pairs 1 and 2 was generated by repeatedly applying a block of 1001 randomized loads of 11 different magnitudes shown schematically in Figure 2. The details were arranged on the girder so that each type of detail would develop fatigue cracks during the experimental

studies. Table 1 provides a summary of the minimum, maximum, and effective stress range for each detail on the eight test girders. Also provided is the frequency, γ, that each detail exceeded its constant amplitude fatigue limit. The magnitude and frequency of the stress range block at each of the 17 details on Girder Pairs 1 and 2 are given in Appendix A, Tables A1 and A2. Only cover plate details 1 and 17 and stiffener detail 9 had stress range levels that differed other than the maximum overload cycle for Girder Pairs 1 and 2 (because of change in cover plate length and web gap). The tenth highest load in the spectrum was close to the fatigue limit of the web and stiffener details. A single overload was included in the spectrum at set exceedance rates corresponding to the block length. For the first and second pairs of girders, this rate was 0.1 percent of the variable cycles.

The third pair of girders was subjected to a variable amplitude stress spectra generated by repeatedly applying a block of 10,001 randomized loads at 16 different magnitudes, as shown in Figure 3. The fourth pair of girders had the lowest six blocks of stress range truncated from the wide-band Rayleigh-type spectrum. The resulting skewed spectrum is shown in Figure 4. Tables A3, A4, and A5 (Appendix A) show the magnitude and frequency of the stress range blocks used for the 17 details on Girder Pairs 3 and 4. This resulted in a single overload for Girder Pair 3 at an exceedance rate of 0.01 percent. The truncated exceedance rate for Girder Pair 4 increased to 0.05 percent.

All specimens were designed to crack first at the web attachment details, second at the stiffeners, and finally at the cover plates. This approach would permit the web cracks to be arrested without expensive repair procedures, so that the test could continue.

TEST PROCEDURES

All girders were tested in four-point bending, as illustrated in Figure 1. The test setup for Pair 3 is shown in Figure 5. The setups for the tests were all similar. Girder Pairs 1 and 2 were tested on the dynamic test bed in Fritz Engineering Laboratory. Girder Pairs 3 and 4 were tested in the multidirectional loading laboratory of the NSF Engineering Research Center for Advanced Technology for Large Structural Systems (ATLSS). All the test setups distributed the jack load to the test girder with a spreader beam.

For Girder Pair 1, a diaphragm consisting of W14X22 rolled section was bolted to the connection plate with its free end supported against vertical motion at the test frame column during cyclic loading of the test specimens. This configuration can be seen in Figure 6. The bottom flange of the test girder was restrained against rotation by means of a rolled section strut, simulating a flange embedded in a concrete deck or the restraint found at a support. The in-plane vertical deflection of the girder from the applied loads causes the connection plate to be forced out-of-plane by the resisting moment developed at the diaphragm connection. This setup models the differential displacement of adjacent bridge girders and the resulting distortion at diaphragm locations in the negative moment region and at supports.

The W14X22 diaphragm created large cyclic stresses in the web gap and early cracking. As a result, small turnbuckles were used on the second pair to obtain smaller stresses in the web gap. Figure 7 shows the two out-of-plane test setups. The two pairs that were used for out-of-plane testing had one strain gauge located at detail No. 8 controlling the horizontal strains. Four more strain gauges were located in the web gap to determine the strain distribution in the gap created by the out-of-plane distortion. The third and fourth pairs of girders had two strain

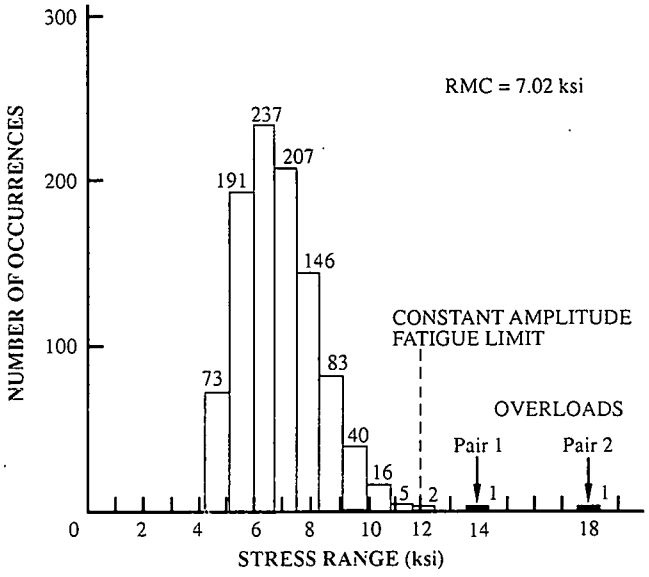

Figure 2. Stress range spectrum at stiffener details 8 and 10 for Girder Pairs 1 and 2, γ = 0.001.

TABLE 1. Summary of stress range characteristics for the welded details

Girder(s)		Cover Plate	Web Attachments						Stiffeners	
		1	2	3	4	5	6	7	8	9
		17	16	15	14	13	12	11	10	
Pair #1	$S_r$min [ksi]	1.30	0.85	1.08	1.10	1.29	1.34	1.51	4.37	4.37
	$S_r$max [ksi]	4.15	2.71	3.47	3.52	4.14	4.29	4.84	14.0	14.0
	S_{re} [ksi]	2.07	1.36	1.74	1.76	2.08	2.15	2.42	7.02	7.02
	γ %	6.4	0.1	**0.8**	0.8	6.4	**14.7**	**29.3**	0.1	**0.1**
Pair #2	$S_r$min [ksi]	2.03	0.85	1.08	1.10	1.29	1.34	1.51	4.37	3.52
	$S_r$max [ksi]	8.34	3.49	4.46	4.52	5.32	5.51	6.22	18.0	14.52
	S_{re} [ksi]	3.25	1.36	1.74	1.76	2.08	2.15	2.42	7.02	5.66
	γ %	**73.7**	**0.1**	**0.8**	**0.8**	**6.4**	**14.7**	**29.3**	**0.1**	**0.1**
Girder 3W	$S_r$min [ksi]	1.38	0.91	1.16	1.18	1.38	1.43	1.62	4.69	4.69
	$S_r$max [ksi]	4.44	2.90	3.71	3.77	4.43	4.59	5.18	15.0	15.0
	S_{re} [ksi]	1.99	1.29	1.66	1.69	1.98	2.05	2.31	6.70	6.70
	γ %	**4.3**	0.01	0.3	0.3	**4.3**	**4.3**	**13.2**	0.01	0.01
Girder 3E	$S_r$min [ksi]	1.16	0.76	0.97	0.98	1.16	1.20	1.35	3.91	3.91
	$S_r$max [ksi]	3.70	2.42	3.09	3.14	3.70	3.83	4.32	12.5	12.5
	S_{re} [ksi]	1.66	1.08	1.38	1.41	1.65	1.71	1.93	5.59	5.59
	γ %	0.3	0	0.01	0.01	0.3	**0.7**	**2.3**	**0.01**	**0.01**
Pair #4	$S_r$min [ksi]	3.71	1.55	1.98	2.01	2.37	2.45	2.77	8.00	8.00
	$S_r$max [ksi]	7.41	3.10	3.96	4.02	4.73	4.90	5.53	16.0	16.0
	S_{re} [ksi]	4.09	1.71	2.18	2.22	2.61	2.70	3.05	8.83	8.83
	γ %	**100**	**0.05**	3.4	**6.5**	**36.5**	**36.5**	**100**	0.05	0.05

γ = percentage of CAFL exceedance

Cracks developed at one or both of these details when **Bold Faced.**

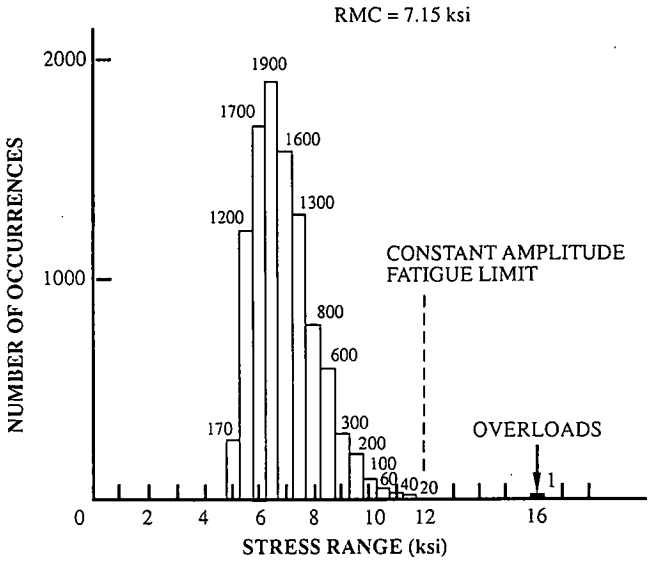

Figure 3. Stress range spectrum at stiffeners 8, 9, and 10 for Girder 3, γ = 0.0001.

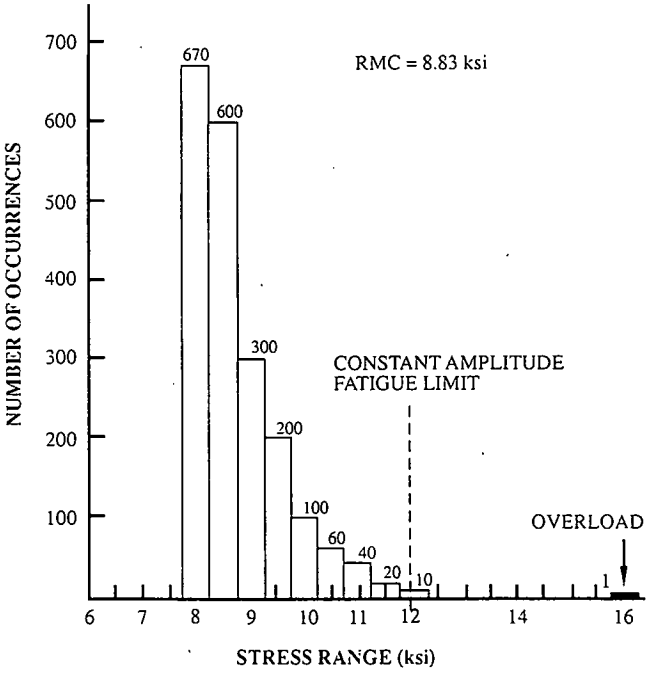

Figure 4. Stress range spectrum at stiffeners 8, 9, and 10 for Girder Pair 4, γ = 0.0005.

gauges located at the midspan of the girder, 3 in. off the centerline on the bottom flange. Servo-hydraulic actuators and controllers were used to produce the random variable loading. For Girder Pairs 1 and 2, the system was automated by an MTS 4021 controller, using a triangular waveform and the internal program, to control the actuator displacements.

The pairs tested in the multidirectional laboratory used the Vickers control system with digital servo values to produce a haversine waveform. Control was provided by a personal computer.

Static calibration tests were carried out on all girders to provide the relationship between strain and displacement. Measurements of the response wave amplitude were obtained with a Nicollet waveform storage oscilloscope to provide dynamic calibrations. Short programs of constant amplitude stress were generated to determine the necessary response time of the actuators, and to achieve the required strain range and the maximum frequency the system could handle without altering the waveform. The fatigue tests for Pairs 1 and 2 were conducted at an average frequency of 2.7 Hz. The third and fourth pairs were tested at average frequencies between 4 and 5 Hz.

RETROFITTING PROCEDURES

The fatigue cracks that formed at the various details always developed at a weld toe or ground region as surface cracks. With the exception of Girder Pair 1, which was subjected to out-of-plane distortion at the center stiffener (No. 9) web gap, cracks were first detected at the web attachments. Generally, the cracks were between 0.5 and 1 in. (12 to 25 mm) long at the time of detection. Initially, 1-in. (25-mm) holes were drilled at the lower crack tip after the crack extended through the web thickness. This arrested the crack extension toward the tension flange. If the crack reinitiated from the crack arrest hole, a larger hole was installed, which often included the original hole.

The cracks that formed at the center stiffener of Girder Pair 1 occurred quickly and were detected after about 50,000 cycles of random load. Holes were initially drilled to arrest the crack growth at about 260,000 cycles. The cracks reinitiated several times and were drilled again to arrest crack growth. It was finally necessary to remove the diaphragms to prevent out-of-plane movement. One stiffener detail on beam 2N developed a crack that propagated into the tension flange. It was thus necessary to add splice plates and clamps, as well as to drill a hole, in order to prevent further crack growth.

No cracks were detected during the test at cover plates with transverse end welds (Girders 1 and 3). One small crack was detected at the unwelded cover plate on beam 3E after the test was completed and the detail was examined destructively. The girders with longer cover plates and with no end welds formed cracks at one or both longitudinal weld terminations where the cyclic stress was high. These cracks were not arrested during the tests.

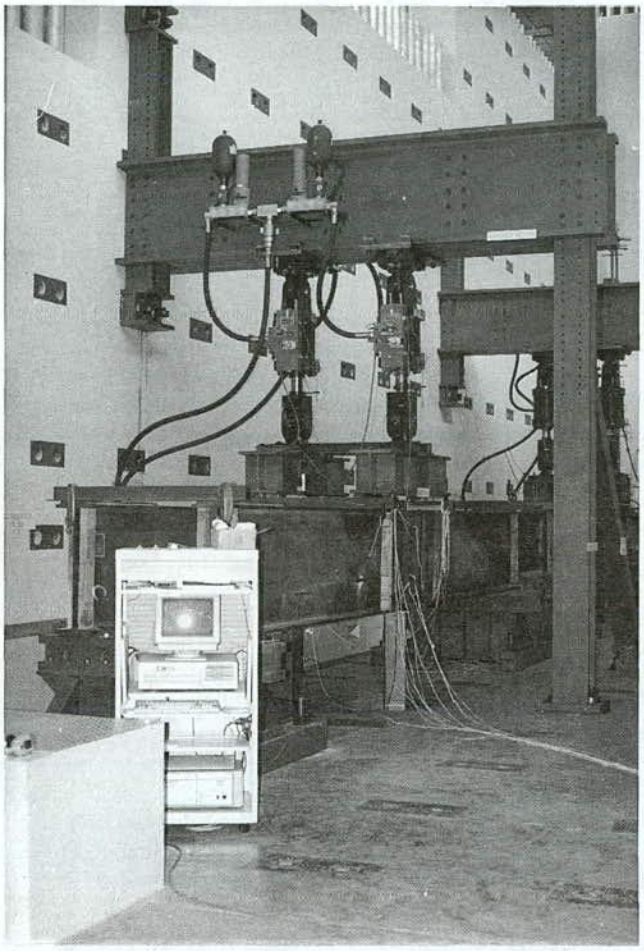

Figure 5. Test setup.

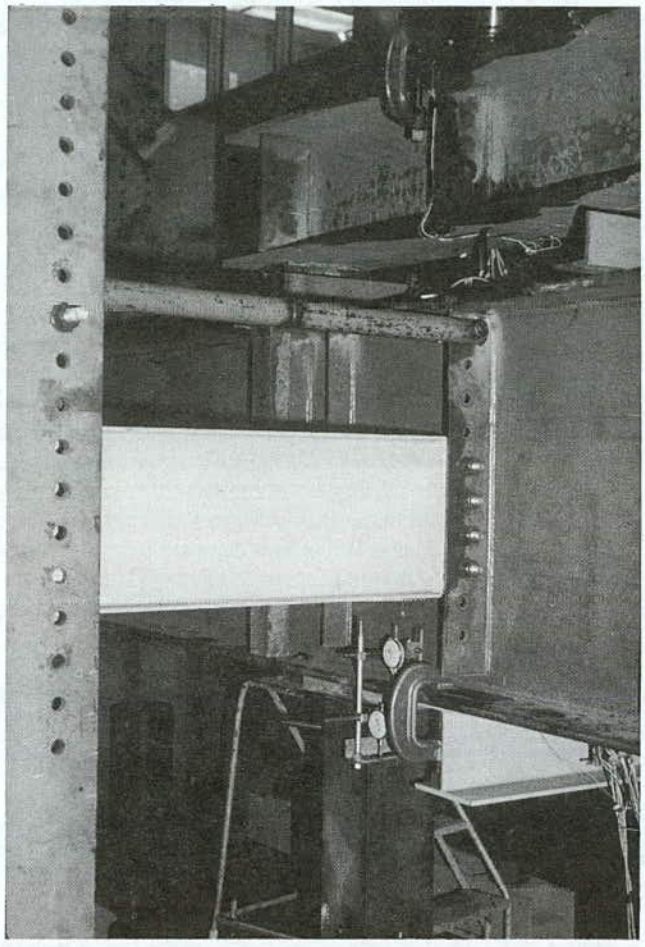

Figure 6. Diaphragm for distortion induced tests.

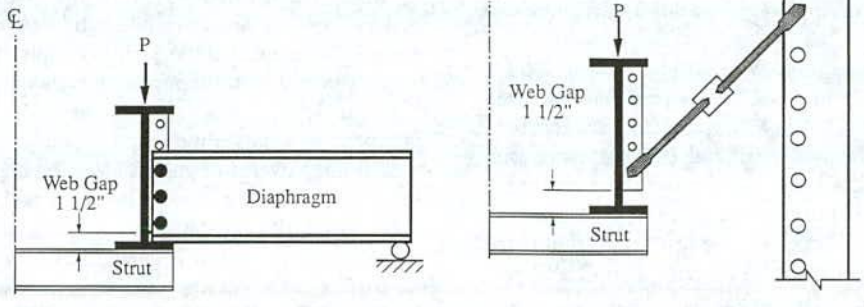

Test Setup for Distortion in Girder Pair 1

Test Setup for Distortion in Girder Pair 2

Figure 7. Test setup for distortion induced web gap cracking for Girder Pairs 1 and 2.

CHAPTER 2

FINDINGS

The findings of NCHRP Project 12-15(5) are summarized in this chapter. A detailed evaluation and documentation of the test results is given in Chapter 3. A detailed review and evaluation of available test data on full-scale, welded steel specimens subjected to either constant cycle or random variable loading was provided in *NCHRP Report 286* (*5*) and will not be repeated here. Since publication of that report in 1986, a study was also commenced by FHWA at the University of Pittsburgh, the University of Maryland, and at Turner-Fairbanks Highway Research Center on Variable Amplitude Load Fatigue (DTFH61-86-C-00036). That study, which is still underway, involves small specimen tests on stiffener (nonload-carrying fillet welds) details; and full-size beam tests on Category C stiffener details, Category D attachments, Category E web gusset plates, and Category E′ cover plates. None of those test results are reported herein. A review of available variable loading test data is provided in Reference *6*.

FATIGUE BEHAVIOR OF WEB ATTACHMENTS

Of the 48 welded web attachments with each having two possible crack initiation sites (and on both sides of the web), 35 different fatigue cracks developed. The effective stress range at the cracked details considering all stress cycles varied from a low value of 1.36 ksi (9.4 MPa) to a high value of 3.05 ksi (21 MPa). The highest S_{re} occurred on Girder Pair 4 where the lowest stress cycles were truncated from the spectrum (see Figure 4). Except for three details, the fatigue resistance equaled or exceeded the fatigue resistance provided by a direct extension of the Category E′ fatigue curve plotted as a log-log relationship (exponential model).

Using the Category E′ constant cycle fatigue limit of 2.6 ksi (17.9 MPa) as reference, these cracks developed when the peak stress range exceeded this level at frequencies between 0.01 percent and 70 percent (α = 0.0001 and 0.70). Hence, web attachment Category E′ details are likely to experience fatigue cracking when subjected to infrequent large stress cycles in long life fatigue loading (near 10^8 cycles). The test results continued to confirm the observations made in *NCHRP Report 267* that all stress cycles contribute to fatigue damage when the constant cycle fatigue limit is exceeded. A straight line extension of the Category E′ fatigue-resistance curve below the fatigue limit was a reasonable lower bound to the fatigue test data.

One detail (4E16) was found to have a very low fatigue resistance with fatigue cracking detected after 14×10^6 cycles at an effective stress range of 1.71 ksi (11.8 MPa). Examination of the crack surface showed that an unusually large initial weld toe defect existed as a gouge. The defect was about 0.13 in. (3.3 mm) deep. The defect in question was unusual as it appeared to be related to an undercut in the web plate and overlap of the weld. The size of the defect is about an order of magnitude larger than normal at a weld toe. It appeared to be an extreme condition not normally present in fabricated structures. One other web attachment detail (2N02) was below the Category E′ resistance curve at an effective stress range of 1.36 ksi (9.4 MPa). It was retrofitted at 94.3 million cycles.

FATIGUE BEHAVIOR OF TRANSVERSE STIFFENERS AND CONNECTION PLATES

Of the 20 details subjected to long-life random variable loading (104 to 120 million cycles for Girder Pairs 1 through 3, and the truncated stress range spectrum with 34.7 million cycles for Girder Pair 4), only four developed fatigue cracks when the effective stress range was below the constant cycle fatigue limit. Two cracks occurred in Beam 2N at detail 8 and 10 cracks occurred under variable loading. The other two cracks on Beam 3E developed during 5 million cycles of constant amplitude stress range at 12.5 ksi (86 MPa), which was applied after 104 million variable amplitude cycles. During the variable amplitude loading of beam 3E, only 11,000 cycles had exceeded the constant amplitude fatigue limit of 12 ksi (83 MPa).

The test results suggest that stiffeners are not likely to experience fatigue cracking in highway bridge structures when few cycles (< 0.1 percent) exceed the fatigue limit. When cracks did form under the variable loading, all test data equaled or exceeded the fatigue resistance provided by an extension of the Category B line at a slope of three to one on a log-log plot.

Two midspan stiffeners on the first pair of beams were subjected to out-of-plane distortion, which resulted in large web gap stresses that exceeded the yield strength of the web plate. This resulted in cracks forming under variable amplitude loading at approximately 50,000 random load cycles. The second pair of girders with the larger web gap [4½ in. (114 mm)] was subjected to 20 million cycles of variable loading and out-of-plane distortion. Two small cracks were detected at the distorted stiffener.

The results demonstrated that out-of-plane distortion can result in cracking that in turn is deleterious to the fatigue strength of the stiffener. The results were consistent with the experimental data reported in *NCHRP Report 336* (*7*).

FATIGUE BEHAVIOR OF COVER PLATES

The cover plate details had two end weld conditions: one where the welds were wrapped completely around the cover plate end (Girder Pairs 1 and 3) and the other where the two longitudinal welds were terminated (Girders Pairs 2, 3, and 4). Several of the longitudinal welds had the end weld termination

ground at their fabrication. All end-welded details had an effective stress range below the estimated constant cycle fatigue limit of 2.6 ksi (17.9 MPa). Only the unwelded details on Girder Pair 3 had an effective stress range below 2.6 ksi (17.9 MPa). One small crack was detected at one of these unwelded details $\simeq 1/8$ in. (3 mm) after 104 million cycles. All test data exceeded the lower bound resistance provided by the Category E′ line extended using a slope of three to one on a log-log plot.

At cover plates with no end welds (Girders 2 and 4), all eight details developed fatigue cracks as the effective stress range was above the estimated constant cycle fatigue limit [3.25 ksi and 4.09 ksi (22.4 MPa and 28 MPa)].

RETROFITTING PROCEDURES DURING THIS STUDY

Placement of holes at the crack tips in the girder web was an effective means of arresting fatigue cracks originating at a weld toe on the web plate. It was observed that the peak stress range in the cycle must satisfy the relationship $\Delta K/\sqrt{\rho} \leq 4\sqrt{\sigma_y}$ if the hole was to prevent the crack from reinitiating. In this relationship, ΔK is the stress intensity factor range for a through-thickness crack, ρ is the radius of the drilled hole, and σ_y is the yield stress of the web plate.

At the transverse connection plate that was deformed out-of-plane, holes could not prevent the crack from reinitation.

CHAPTER 3

INTERPRETATION, APPRAISAL, AND APPLICATION

This chapter contains a summary description, interpretation, and appraisal of the analytical studies and laboratory experiments. The fatigue characteristics of three types of welded details were examined under random variable loading. One detail was the transverse stiffener. Limited information was also obtained on a transverse connection plate at midspan, which simulated diaphragm connection plates. The second detail evaluated was the web gusset plate fillet welded to the girder web. The attachment geometry (1 in. × 12 in.) resulted in the gusset being classified as a Category E′ detail. The third detail was the cover plate, which also was classified as a Category E′ detail as the flange thickness exceeded 0.8 in. (20 mm).

Each of the test details was subjected to a random variable amplitude loading that resulted in some cycles exceeding the constant amplitude fatigue limit (CAFL). The three details were installed on girders such that different stress range levels could be achieved from the geometry. The web attachment details were located such that several would develop fatigue cracks before the cover plate details. This would allow the web cracks to be quickly retrofitted so that the long-life testing could resume. In this manner, a single beam could ideally provide experimental data on up to 17 details. This was highly desirable considering the test time to achieve 100 million cycles.

The primary procedure used to arrest crack growth and extend the fatigue life of a detail was to install drilled holes at the crack tips. On the first pair of girders that developed early cracking at the diaphragm connection plate detail, other supplementary procedures were also carried out such as peening the weld toe and grinding.

ANALYTICAL ASSESSMENT

Linear-elastic fracture mechanics has become a recognized tool to assess fatigue crack growth at welded details.

The Paris Power Law is generally used to relate fatigue crack extension, da/dN, to the range of stress intensity factor, ΔK, and is given by:

$$\frac{da}{dN} = C\ \Delta K^n \tag{1}$$

The best estimate for the upper bound for fatigue crack growth rate in bridge steels and weldments is given by:

$$\frac{da}{dN} = 3.6 \times 10^{-10}\ \Delta K^{3.0} \tag{2}$$

where the units at a and K are inches and ksi $\sqrt{\text{in.}}$, respectively. This relationship will be used in the fatigue crack growth model. The assumption is made that cycle interaction does not occur. This implies that crack growth acceleration or retardation does not result from cycle overloads or underloads to the degree that the crack growth rate changes significantly from the assumed values over the life of the detail. The experiments to be modeled have load cycles applied from a constant minimum load level and as individual load cycles. No cycle addition or superposition of smaller stress cycles occurred. In addition, the load cycles were classified in a random fashion over the spectrum.

The calculation of the stress intensity range, ΔK, for welded bridge details, such as cover plate terminations and web attachments, can be related to the idealized case of a central through crack in an infinite plate by the application of appropriate stress field correction factors (*8–10*). The generalized stress intensity range is given by:

$$\Delta K = F(a)\ S_r \sqrt{\pi a} \tag{3}$$

where $F(a)$ is the product of all applicable correction factors as a function of crack length, a, and is given by:

$$F(a) = F_e F_s F_w F_g \tag{4}$$

where

F_e = elliptical crack shape correction
F_s = free surface correction
F_w = finite width correction
F_g = stress concentration correction

The general approximation for the stress gradient correction factor, F_g, that was used for the three details was of the form (*1, 11, 12*):

$$F_g = \frac{K_{tm}}{1 + G\alpha^{\beta}} \tag{5}$$

where G and β are dimensionless constants; α is the ratio of crack size to the web plate (stiffener and gusset) thickness or flange plate (cover plate), a/t; and K_{tm} is the maximum stress concentration factor at the weld toe.

Fatigue crack propagation under variable amplitude loading was simulated using the crack growth models in a stepwise fashion, as governed by the crack growth threshold. For each stress cycle in the spectrum, the threshold crack size was determined. Figure 8 shows the spectrum used for a typical detail. As the magnitude of the stress cycle increases, the threshold crack size decreases. The effective stress range (RMC) was then calculated from the stress cycles in the spectrum that had a crack threshold size below the assumed initial crack size (0.03 in., 0.75 mm) for each detail (*9, 13*). Crack propagation calculations

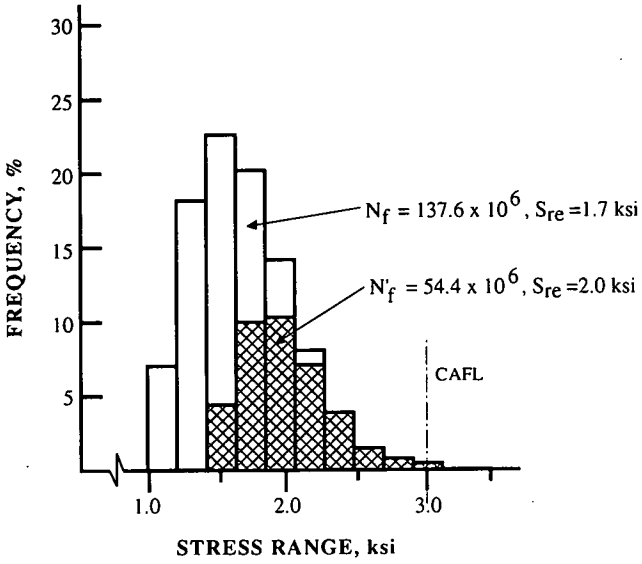

Figure 8. Web attachment cycle life, detail 3.

were made with this effective stress range by integrating from the initial crack size to the threshold crack size of the next lowest stress cycle in the spectrum. This gave the number of cycles required to propagate the crack to the next lowest noncontributing stress cycle. A new crack growth calculation was made with a lower effective stress range value determined from a new stress spectrum that included the next lowest stress cycle. The integration was performed from the crack threshold size of the smallest stress cycle in the new truncated spectrum to the threshold crack size of the next lowest stress cycle. This procedure was repeated until the crack penetrated the plate thickness.

Although the full stress range spectrum is continuously applied to the detail, for the purpose of this study it is assumed that only a portion of the stress cycles in the spectrum may actually contribute to crack growth in the high-cycle, long-life regime as governed by the crack threshold. By integrating the crack growth model in increments, the number and distribution of stress cycles that contribute to crack propagation during the total life of the welded detail can be determined. The total number of contributing cycles is referred to as the effective cycle life, N_f'. The value of the effective cycle life is always less than the nominal cycle life, N_f, determined by the full spectrum. In addition, the effective stress range for the truncated spectrum results in a higher value, S_{re}'.

The crack growth simulation was performed on the web attachments and cover plate details. Figure 9 shows the results obtained for the web attachments using a stress concentration, K_{tm} = 7; an initial crack size a_i = 0.03 in. (0.75 mm); and a crack growth threshold of 2.75 ksi $\sqrt{\text{in.}}$ (3.0 MPa $\sqrt{\text{m}}$). The predicted result for the fatigue crack growth model considering only contributing stress cycles is shown as the short-dashed line. The predicted result using all stress cycles and ignoring the crack growth threshold is shown as the long-dashed line in Figures 9a and 9b. Both predicted relationships shown in Figure 9b are bounded by the Category E and E′ resistance curves. The spectrum corresponding to these two conditions is shown in Figure 8, where the contributing stress cycles are shown by the cross-hatched areas.

The predicted results indicate that the smaller stress cycles' contribution to fatigue damage is dependent on the crack growth threshold. In general, the analysis indicates that including the noncontributing stress cycles in the fatigue life estimate is a conservative procedure.

EXPERIMENTAL RESULTS ON WEB GUSSET PLATES

The experiments were carried out with paired girders, as illustrated in Figure 5. Each girder was independently loaded with a single jack that was distributed to the girder with a spreader beam. All of the welded details attached to the web plate provided visual indication of the residual stress fields introduced by the fabrication process. Figure 10 shows yield lines that developed when the stiffeners and gusset plates were welded to the girder web. It is apparent that yield level residual stresses are introduced at the weld toe of these attachments.

The gusset plate details were all located in the shear spans and were subjected to cyclic in-plane stresses. The applied stresses were measured by strain gages and correlated by bending

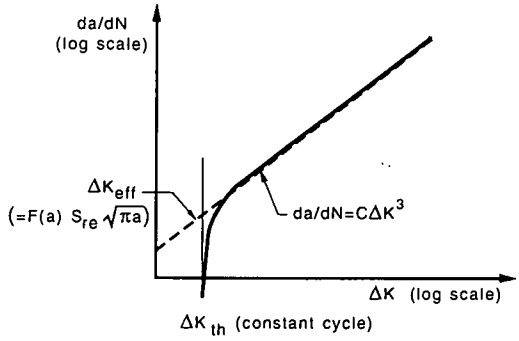

(a) Crack growth relationship for constant cycle loading and random variable loading.

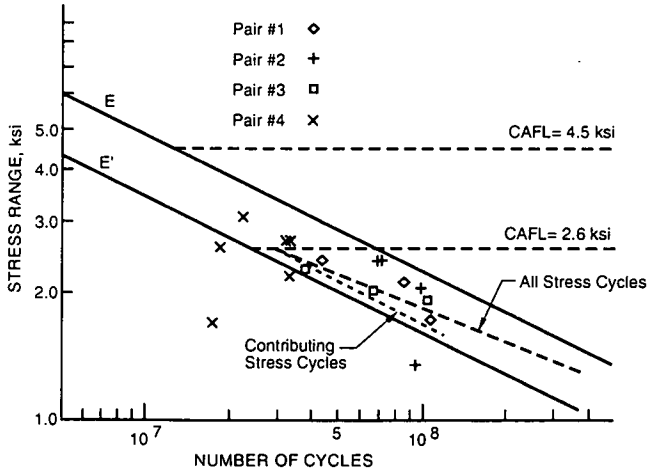

(b) Comparison of predicted fatigue resistance under variable loading with test data.

Figure 9. Predicted fatigue resistance compared with design resistance curves and test data for web attachments.

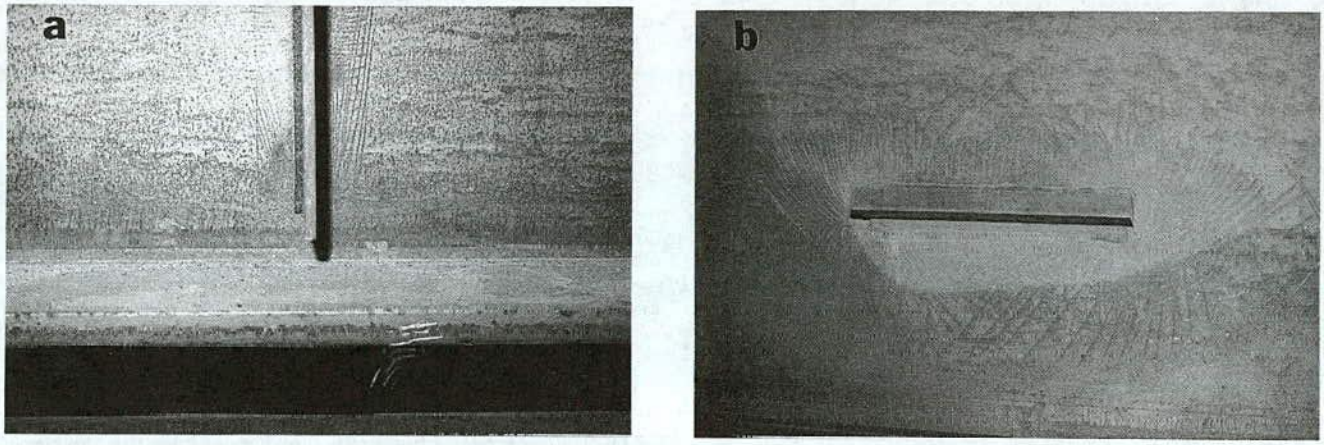

Figure 10. Yield lines in mill scale adjacent to welded details confirm existence of residual stresses. (a) Stiffener detail showing yield lines after welding. (b) Web gusset detail showing yield lines after welding.

TABLE 2. Number of cycles to first detected crack

Girder		1N	1S	2N	2S	3W	3E	4W	4E
Total Cycles		107.2	107.2	120	120	104	109	34.7	34.7
Detail									
Coverplate	1	-	-	78.5^{+}	72.1^{+}	-	-	20.9^{+}	20.9^{+}
	1	-	-	72.3^{+}	72.3^{+}	-	-	-	-
	2	-	-	72.9	72.1	-	-	-	-
	3	-	100.7	-	75.8	-	-	-	-
Web	4	-	-	-	96.7	-	-	-	-
attachment	5	-	-	88.5	69.5	-	-	-	19.6
	6	-	81.7	86.9	120.0	-	-	-	19.6
	7	-	-	78.5	65.3	37.8	98.5	-	-
Stiffener	8	-	-	89.5	-	-	109	-	-
	9	0.05*	0.05*	120*	120*	-	109	-	-
	10	-	-	120	-	-	-	-	-
	11	-	43.6	66.7	72.1	-	109	19.6	-
	12	-	-	72.3	-	40.9	109	26.5	-
Web	13	-	-	80.7	72.1	-	-	12.3	19.6
attachment	14	-	-	-	-	-	-	14.0	-
	15	-	-	88.5	99.6	-	-	-	-
	16	-	-	88.5	82.3	-	-	-	14.0
	17	-	-	72.3^{+}	88.1^{+}	104^{+}	-	20.9^{+}	17.4^{+}
Coverplate	17	-	-	-	87.2^{+}	-	-	20.9^{+}	20.9^{+}

* = Distortion induced cracking
- = No crack detected
$^{+}$ = Coverplates without end welds

TABLE 3. Number of cycles to maximum size-cracking criteria (i.e., through thickness or 1 in. long)

Girder		1N	1S	2N	2S	3W	3E	4W	4E
Total Cycles		107.2	107.2	120	120	104	109	34.7	34.7
Detail									
Coverplate	1	-	-	120	120	-	-	34.7	34.7
	1	-	-	120	120	-	-	-	-
	2	-	-	94.3	120	-	-	-	-
	3	-	107.2	-	120	-	-	-	-
Web	4	-	-	-	>120	-	-	-	-
attachment	5	-	-	>120	>120	-	-	-	>34.7
	6	-	86.0	>120	>120	-	-	-	32.0
	7	-	-	120	69.5	37.8	104	-	-
Stiffener	8	-	-	89.5	-	-	109	-	-
	9	0.26*	0.26*	>120*	>120*	-	>109	-	-
	10	-	-	120	-	-	-	-	-
	11	-	43.6	71.9	120	-	>109	22.6	-
	12	-	-	120	-	67.2	>109	33.0	-
Web	13	-	-	120	99.6	-	-	18.6	>34.7
Attachment	14	-	-	-	-	-	-	33.0	-
	15	-	-	>120	>120	-	-	-	-
	16	-	-	>120	>120	-	-	-	17.4
	17	-	-	>120	>120	104	-	>34.7	32.0
Coverplate	17	-	-	-	>120	-	-	>34.7	>34.7

* = Distortion-induced cracking
- = No crack detected
> = Crack that did not reach the maximum size cracking criteria.

theory. Tables 2 and 3 summarize the experimental data for all the details. Table 2 shows the cumulative cycles to first detected crack at a detail initiation site. A dash indicates that no cracks developed during the test. Table 3 shows the cycles corresponding to a through-thickness crack in the web plate, which was defined as failure. When the symbol > is shown, it indicates that the crack had not extended through the web thickness so that additional cycles were possible.

Fatigue Behavior of Gusset Plates

During the variable cycle loading, cracking was observed to initiate at the end of the longitudinal weld, as illustrated in Figure 11. As noted earlier, several of the details had the weld end smooth-ground at the time of fabrication. Figure 12 shows the crack that initiated at detail 11 of Beam 1S. The initiation site

is at the longitudinal weld root. This was typical of most smooth-ground weld terminations. Figures 13 and 14 show the crack surfaces of two details. Figure 13 is a view of semielliptical crack with residual life, because the crack has not penetrated through the web thickness. Figure 14 shows a through-thickness crack that was defined as failure.

Detail 16 on beam 4E experienced premature cracking at a low effective stress range as a result of a large initial defect at the weld toe. (See Figure 15). Close examination of the web showed that the surface was ground. Subsequent examination indicated that the detail weld was slightly over a small gouge area, as illustrated in Figure 16. Apparently, this repair was the origin of the crack. The gusset plate welds terminated at this defect, which extended about 0.06 in. (1.5 mm) into the web at the weld toe.

All of the experimental data from the earlier studies (*5*) and this program are summarized in Figures 17 and 18. The test results are compared with the Category E′ fatigue-resistance curve applicable to this detail. Several cracks were detected below the fatigue-resistance curve. The detail with the large initial defect from beam 4E is readily apparent. Most details that developed cracks below the fatigue-resistance curve failed near or slightly above the straight line extension of Category E′ below the estimated constant cycle fatigue limit on the plot of effective stress range.

The exceedance levels of the web attachments and their minimum, maximum, and effective stress range values are shown in Table 1. The exceedance values correspond to the value of 2.6 ksi (18 MPa) assigned to Category E′. This value is based on a fracture mechanics model of a cover-plated beam and appears to be satisfactory for the web gusset detail (*13*). It can also be seen from Tables 2 and 3 that large numbers of cracks developed in Girder Pair 2 compared with Girder Pair 1. Both were subjected to identical exceedance rates for the web details. The primary difference is the level of the peak stress range cycle, $S_{r\max}$. This value was about 29 percent higher in beam set 2 than the peak value in beam set 1.

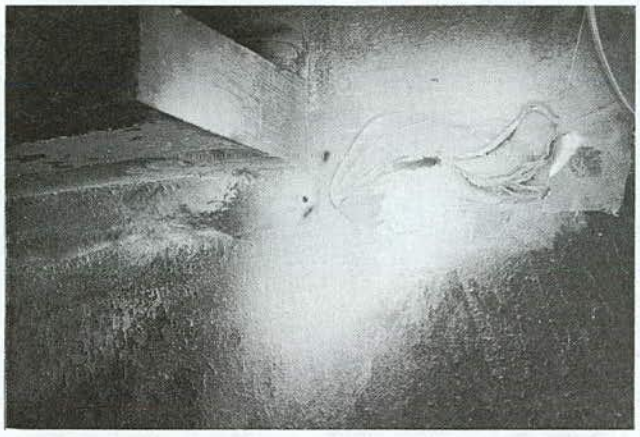

Figure 11. Typical fatigue crack at weld end of gusset plate, detail 7, Girder 3E.

Figure 13. Semielliptical crack at web gusset. (Note crack can exceed web thickness as a result of weld on back surface.)

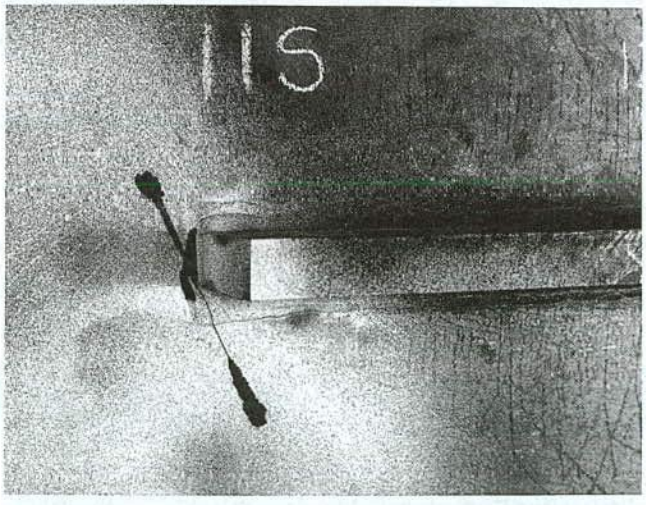

Figure 12. Crack initiated at ground end of gusset plate weld, detail 11, Girder 1S.

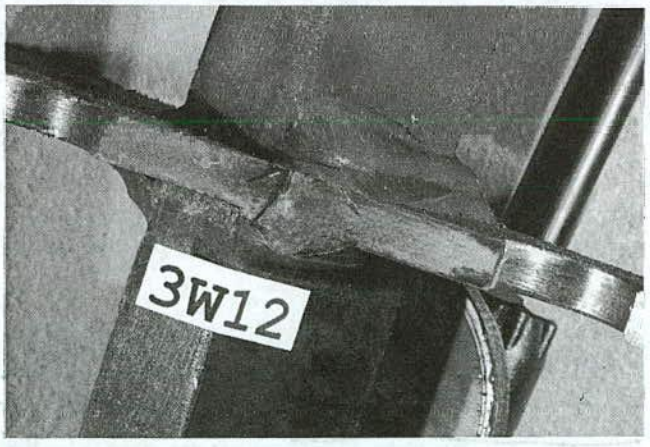

Figure 14. Typical through thickness crack arrested by retrofit holes.

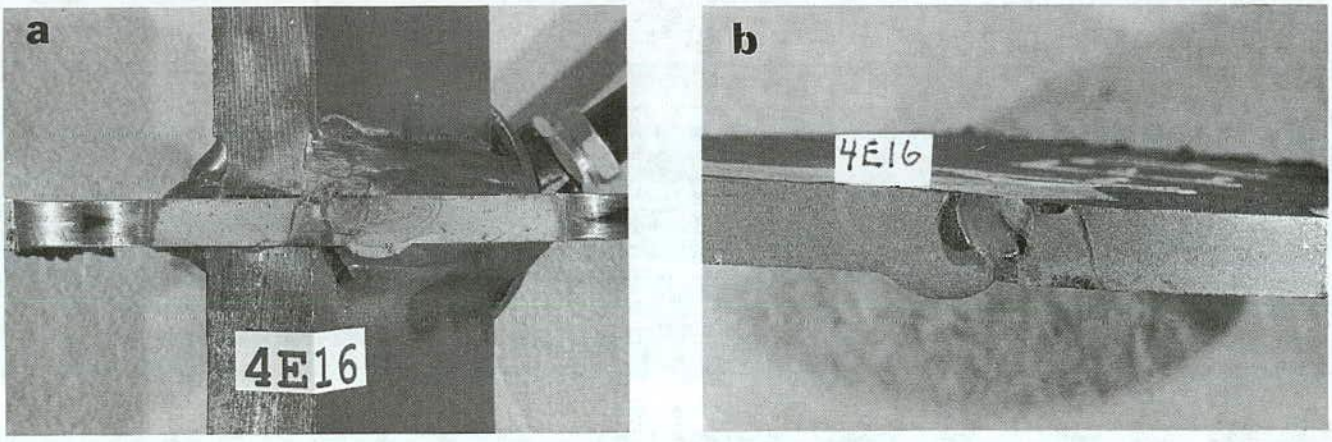

Figure 15. Crack surfaces of web detail 16 Beam 4E with large initial defect. (a) View of crack surface showing origin at weld toe. (b) Close-up view of initial defect in web plate.

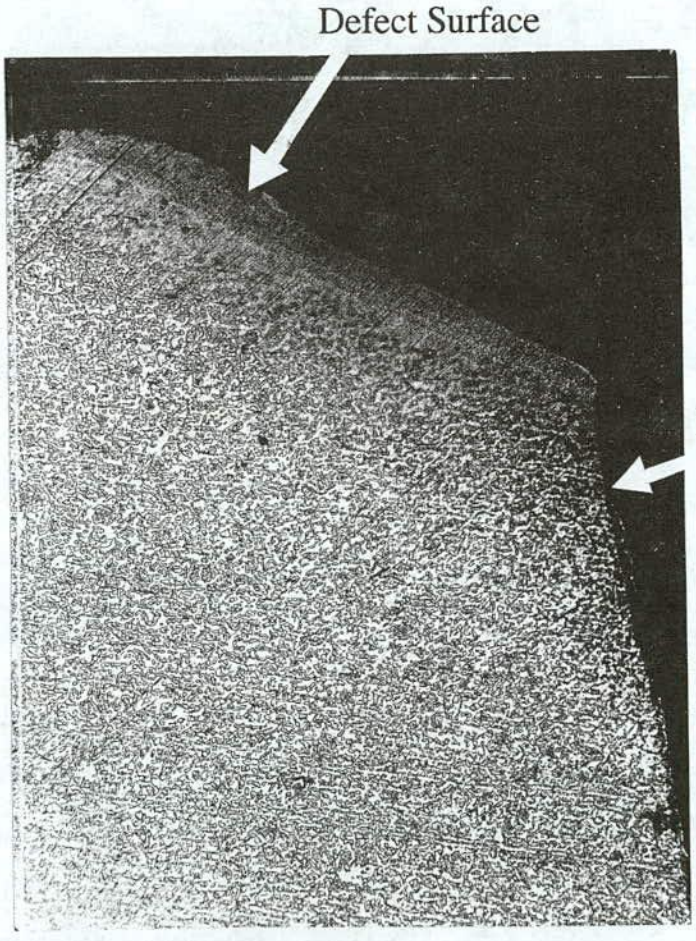

Figure 16. Polished and etched section perpendicular to crack surface showing defect and HAZ @ 40×.

The results also indicate that low exceedance levels will result in fatigue crack growth when the effective stress range is below the constant amplitude fatigue limit. The magnitude of the peak stress range appears to be a major contributor. For Girder Pair 2, one or both details at all exceedance levels experienced cracking (γ = 0.1 to 29 percent). For Girder Pairs 1 and 3E, the exceedance level γ exceeded 0.7 percent before cracking was observed. For Girder Pair 4, the exceedance was 0.05 percent. The results indicate that the peak stress range at the low exceedance levels needs to exceed the constant cycle fatigue limit by about 30 percent if fatigue cracks are to develop. This is likely due to the variability between details on their fatigue limit.

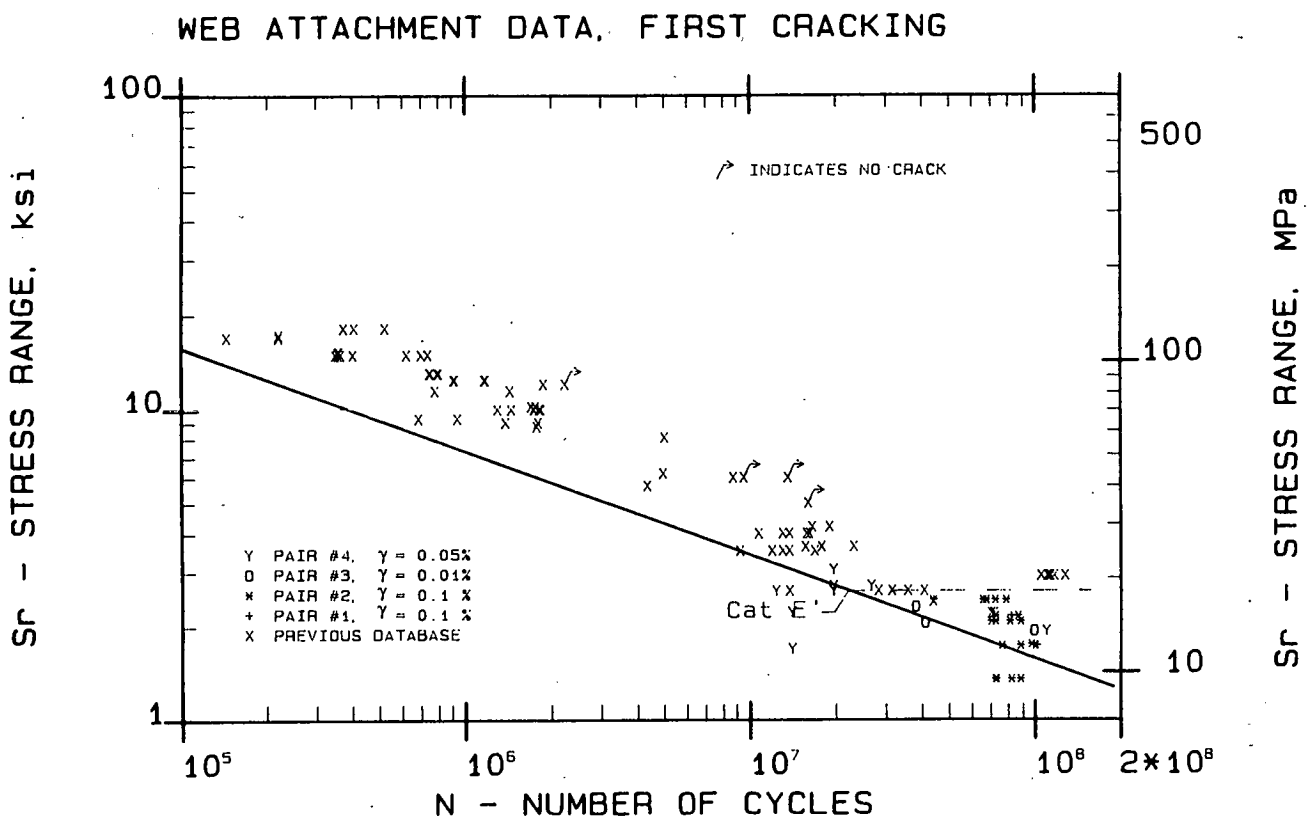

Figure 17. Comparison of web attachment test data at first detected cracking with Category E' fatigue resistance curve.

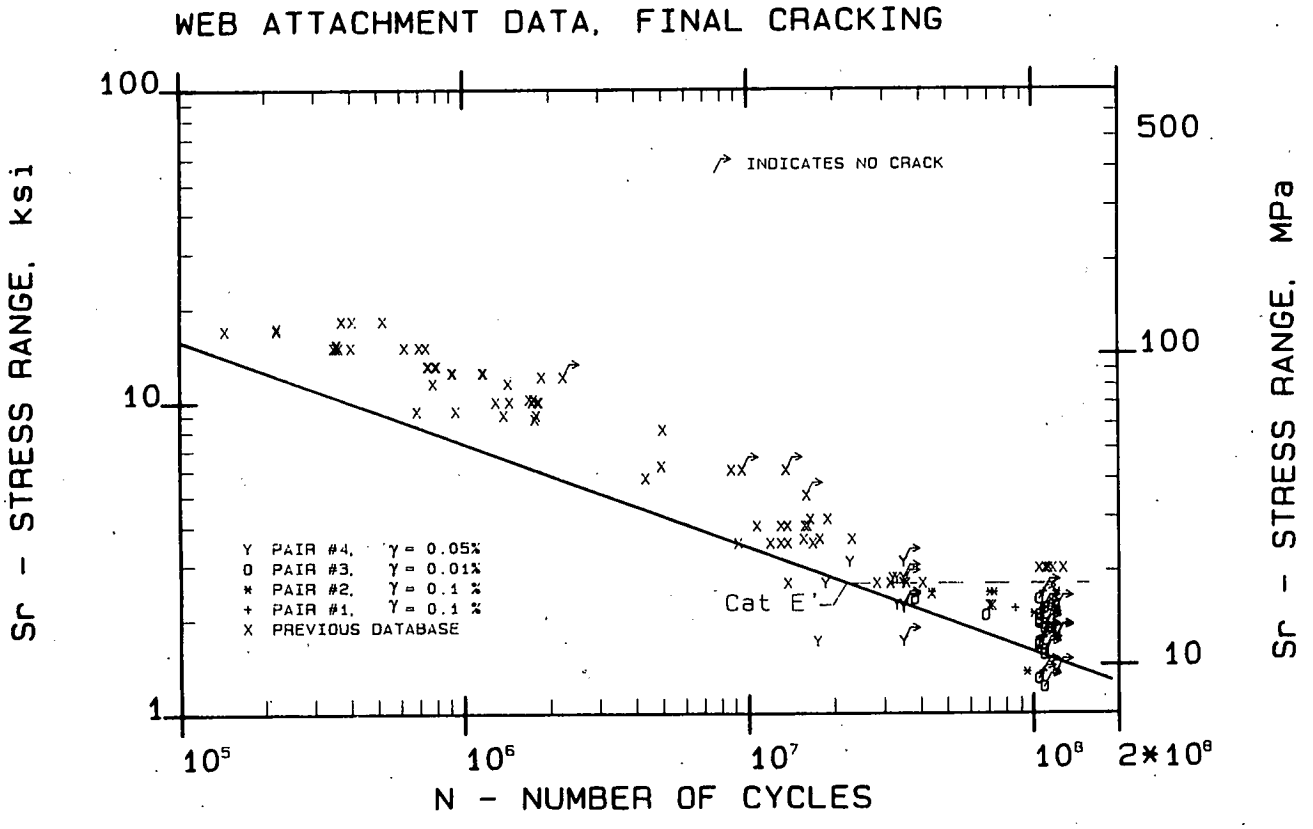

Figure 18. Comparison of the web attachment test data at failure or test termination with Category E' fatigue resistance curve.

Retrofit of Gusset Plate Web Cracks

Retrofit holes were installed at one or both tips of the gusset plate crack after the cracks were through the web thickness. Figure 19 shows the upper drilled hole installed at detail 12, beam 3W, after 67 million cycles. This beam sustained an additional 37 million cycles without additional corrective action. Figure 20 shows the multiple holes installed at detail 7 beam 3W. The initial pair of 1-in. (25-mm) holes were installed after 38 million cycles. The crack reinitiated after 11.7 million cycles and a 2-in. (51-mm) hole was drilled. This was adequate to the end of the test. The retrofit holes were initially sized to satisfy the relationship (*7,14*)

$$\frac{\Delta K}{\sqrt{\rho}} < 4\sqrt{\sigma_y} \tag{6a}$$

(for σ_y in ksi, ρ in in., and ΔK in ksi$\sqrt{\text{in.}}$)

where the hole radius is ρ and the stress intensity factor ΔK was taken as $S_r\sqrt{\pi a_r}$

$$\frac{\Delta K}{\sqrt{\rho}} < 10.5\sqrt{\sigma_y} \tag{6b}$$

(for σ_y in MPa, ρ in meters and ΔK in MPa$\sqrt{\text{m}}$)

where a_r is defined in Figure 21, and the stress range was taken as $S_{r\max}$. Sometimes only a single hole was installed at the bottom end. Once the crack reinitiated from the hole, a second larger hole was installed, as illustrated in Figure 20. Figure 22 shows one of the larger holes cut in the web for Beam 2D at detail 11. This 4.25-in. (105-mm) hole was able to sustain 2 million cycles at $S_{r\max}$ without reinitiation. The effective crack length was 9 in. (229 mm) for this retrofit condition.

The test results for all retrofit holes from earlier studies and this program are plotted in Figure 23. Details of the individual gusset plate results are given in Table 4. The best correlation of the test data was achieved when the maximum stress range in the variable load spectrum was used to assess the resistance to crack reinitiation at the retrofit holes.

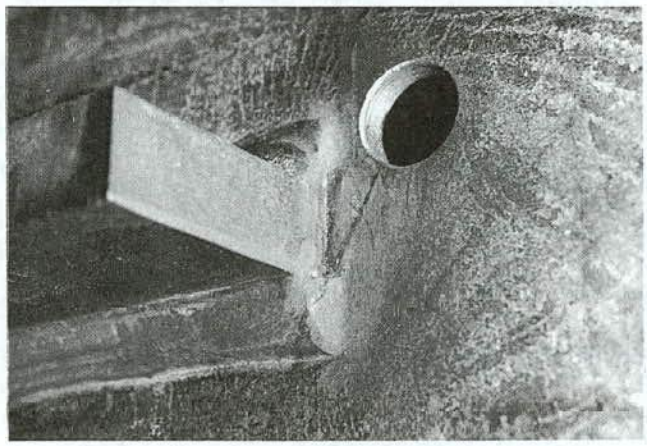

Figure 19. Retrofit hole at top end of crack at detail 12, Beam 3W.

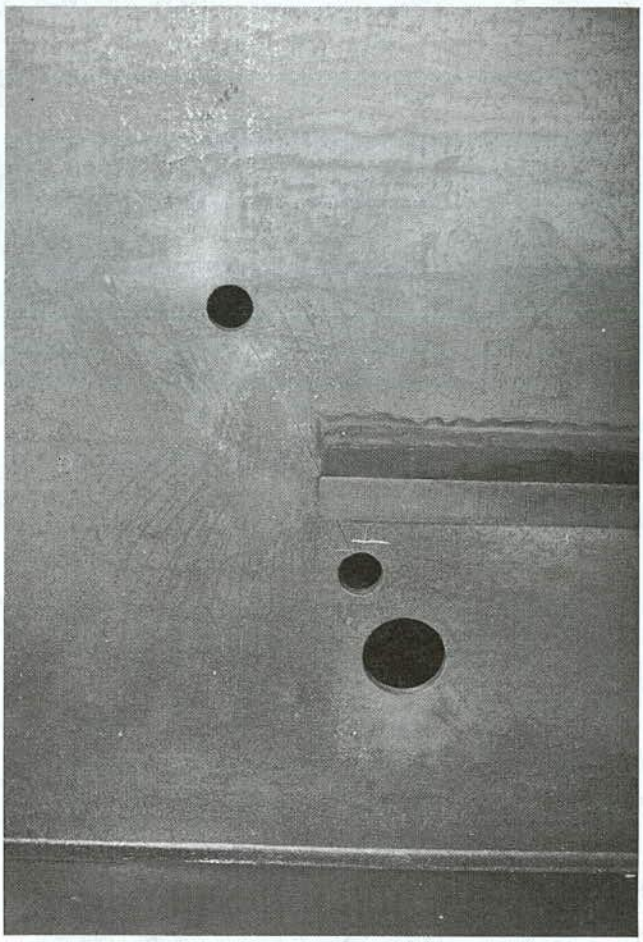

Figure 20. Retrofit holes at detail 7, Beam 3W.

EXPERIMENTAL RESULTS OF TRANSVERSE STIFFENERS

Very little experimental data on stiffener details is available from variable load tests (*5*). Only two data points were available from variable amplitude loading where the effective stress range was below the constant amplitude fatigue limit used for stiffeners (*15*).

Of the 24 stiffener details in this study, four were subjected to out-of-plane distortion (Detail 9 on Girder Pairs 1 and 2), and were not included in the assessment of fatigue resistance. All of the stiffener details were located between the jack load points in a constant moment region. Tables 2 and 3 summarize the stiffener test data for details 8, 9, and 10. Table 2 shows the cumulative cycles at the time the crack was first detected. No cracks developed where a dash mark is shown.

In the case of Girder Pair 1, cracks were detected after only 50,000 variable load cycles as a result of the out-of-plane distortion. For Girder Pair 2 the out of plane distortion was not introduced until after the girders were first subjected to 100 million cycles of in-plane variable loading. Details of the variable load spectrum are provided in Appendix A.

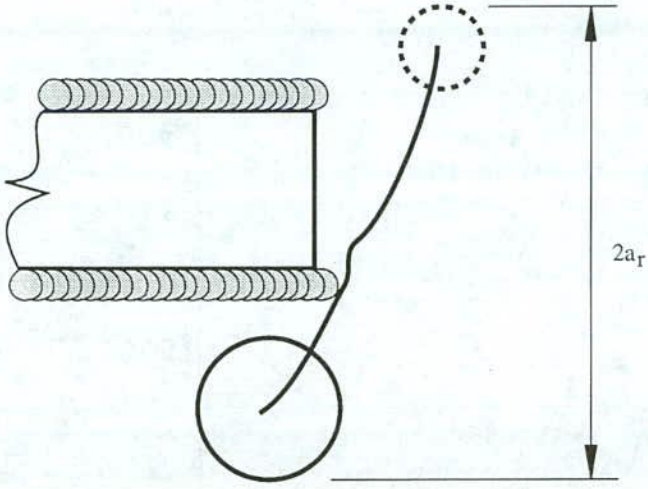

Figure 21. Schematic showing retrofit holes and effective crack length.

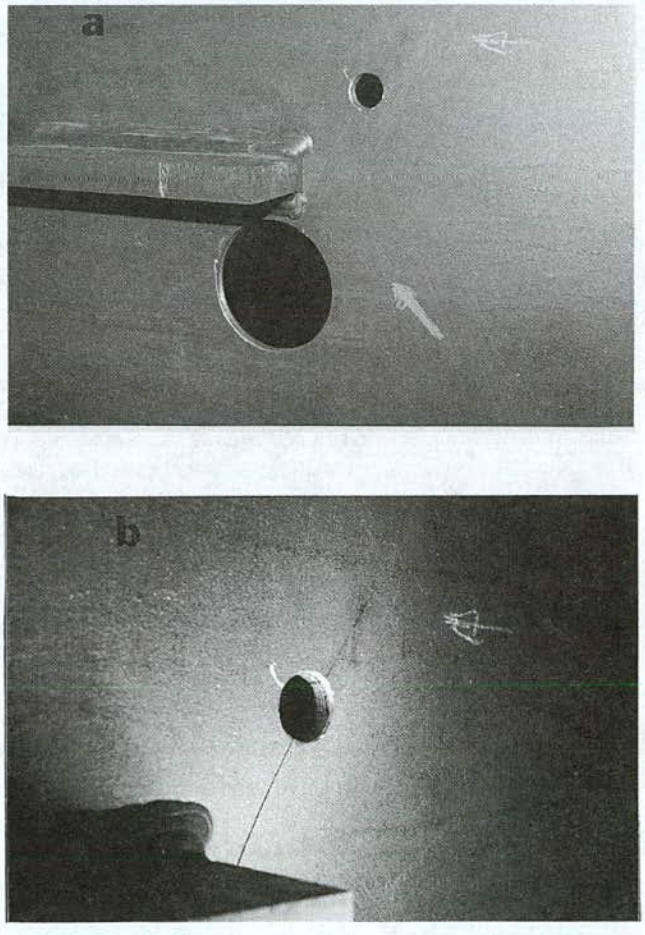

Figure 22. Retrofit holes at detail 11, 2N showing large hole after 2nd retrofit. (a) Large retrofit hole in girder 2N, detail 11; crack reinitiated at top hole. (b) Close-up view of crack at top hole.

TABLE 4. Retrofitted web details; crack size, hole diameter, and cycle data

Detail N°	2a [in.]	Hole Dia. [in.]	Cycles to Retrofit [x 10^6]	Variable Cycles to Reinitiation [x 10^6]	Cycles of S_{rmax} [x 10^3]
1S09*	5.0	1.00	1.03	1.68	1.68
1S09	3.0	1.50	1.03	1.68	1.68
1S11	5.0	2.00	43.6	>107.20	>63.6
1N09*	2.0	1.00	1.03	6.26	5.23
1N09	2.0	1.50	1.03	6.26	5.23
2S07	4.0	1.25	91.1	>120.00	>28.90
2S07	4.0	0.75	91.1	>120.00	>28.90
2N08	8.9	1.00	91.1+	108.00°	16.90
2N11	9.0	4.25	91.1	>120.00	>28.90
2N11	9.0	1.00	91.1	>120.00	>28.90
3W12	5.0	1.00	61.3	>104.00	>4.27
3W12	5.0	1.00	61.3	>104.00	>4.27
3W07	4.0	1.00	37.9	49.60	1.17
3W07	8.0	1.00	51.2	82.80	3.16
3W07	12.0	2.00	51.2	104.00	5.28
3E07	6.0	2.00	105.5	107.10	1600.0
3E07	9.5	6.00	107.1	>109.00	>1900.0
3E07	6.0	2.00	105.5	108.40	2900.0
3E07	13.5	2.00	108.4	>109.00	>600.0
4E16	5.0	1.00	22.4	>34.70	>6.15
4E16	5.0	1.00	22.4	>34.70	>6.15
4W11	6.0	2.00	25.9	>34.70	>4.40
4W11	6.0	1.00	25.9	>34.70	>4.40
4W13	7.0	1.00	22.4	24.70	1.15
4W13	8.5	2.00	25.9	>34.70	>4.40
4W13	7.0	1.00	22.4	28.00	2.80
4W13	11.5	1.00	28.5	>34.70	>3.10

* = Crack in the direction of primary stresses
\+ = Crack tip was not drilled
° = Splice plates added to flange

Fatigue Behavior of Transverse Stiffeners

The stiffener details were only subjected to the overload stress cycle under the maximum load in the variable spectrum (see Figures 2, 3, and 4). Four of the stiffeners on Beams 2N and 3E developed fatigue cracks during the test. In the case of Beam 3E, 5,000,000 constant load cycles at the maximum load level were added after the two girders were subjected to 104 million variable load cycles.

Figure 24 shows the first crack that formed in Girder 2N after 89.5 million cycles. A retrofit hole was drilled to prevent the crack from entering the flange. Only 89,500 cycles exceeded the fatigue limit of this detail during the test for an exceedance of 0.1 percent. The cracks that formed at the other three stiffener details are shown in Figures 25 to 27. The fatigue crack surfaces for details 2N10, 3E08, and 3E09 were exposed after the tests by cooling the segments in liquid nitrogen. Small semielliptical cracks can be seen to have formed and propagated in both of these details about 0.5 in. (12 mm) above the end of the vertical weld.

The test results are summarized in Figure 28. The test data for the four details that developed cracks are plotted two ways. The data are plotted as "z" symbol considering only the maximum stress cycle in the variable spectrum. For details 3E08 and 3E09, the test result is in good agreement with the constant cycle data.

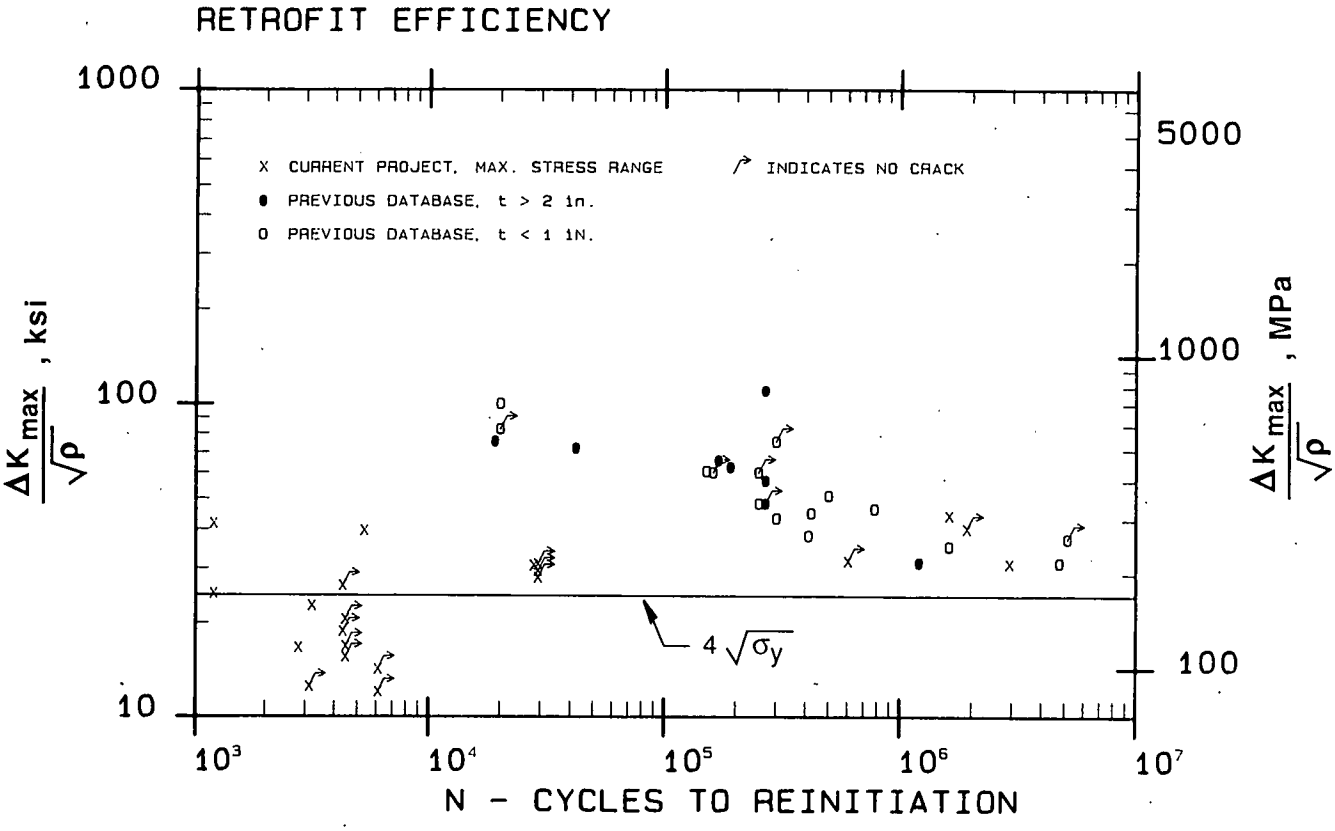

Figure 23. Retrofitted web attachments correlated on the basis of the maximum stress intensity range.

However, for details 2N08 and 2N10, there is no correlation with the constant cycle test data. All stress cycles in the variable load spectrum when plotted at the effective stress range are in reasonable agreement with the extension of the fatigue resistance curve for Category C. The test data for all test points below the assumed constant cycle stress range of 12 ksi (84 MPa), are all well beyond the lower bound fatigue resistance curve.

Only one stiffener detail required retrofitting, as shown in Figure 24. A 1-in. hole was initially drilled at the web flange weld. To minimize reinitiation of the crack into the flange, splice plates were also clamped to the bottom flange (see Figure 24).

It is apparent from the test results that the magnitude of the peak stress cycle was a contributing factor in the development of the stiffener cracks. Girder 2N was subjected to a peak overload stress range of 18 ksi (126 MPa) at the stiffeners. Girder 3E, which also developed cracks, was subjected to a peak stress range of 12.5 ksi (87 MPa) just above the fatigue limit. Altogether, 5,001,100 of these stress cycles were applied. The final crack dimensions are given in Appendix B.

Distortion-Induced Fatigue Cracking

As a secondary study, distortion-induced fatigue cracking at the center connection plate web gap detail was examined under variable amplitude loading. The test program provided an opportunity to examine and evaluate this type of fatigue cracking and possible retrofit methods under long-life conditions.

Figures 6 and 7 show the test girder and diaphragm at midspan. The connection plate was cut short of the tension flange by $1\frac{1}{2}$ in. for Girder Pair 1. A diaphragm consisting of W14X22 rolled section was bolted to the connection plate with its free end supported against vertical motion at the test frame column. This configuration is shown schematically in Figure 7. The bottom flange of the test girder is restrained against rotation by means of a rolled section strut, simulating a flange embedded in a concrete deck or at a support. The in-plane vertical deflection of the girder from the applied loads causes the connection plate to be forced out-of-plane by the resisting moment developed at the diaphragm connection.

Strain measurements taken during static tests, prior to the variable amplitude loading, indicated that the vertical web gap membrane stresses were high. At a static load that produced an in-plane stress of 12 ksi (84 MPa) at the connection plate end equivalent to the constant amplitude fatigue limit, a strain corresponding to 43 ksi (300 MPa) was measured. This distortion-induced stress was approximately 20 percent above the nominal yield stress of the steel. Varying the vertical-bolted position of the diaphragm resulted in no significant changes in the measured web gap stress.

Variable amplitude loading fatigue cracks developed quickly in the web gaps. The initial cracking was first detected at approximately 50,000 cycles, with extensive cracking at 100,000 cycles. The distortion-induced fatigue cracks developed at both the toe of the web-to-flange fillet weld and at the connection plates end, as shown in Figure 29.

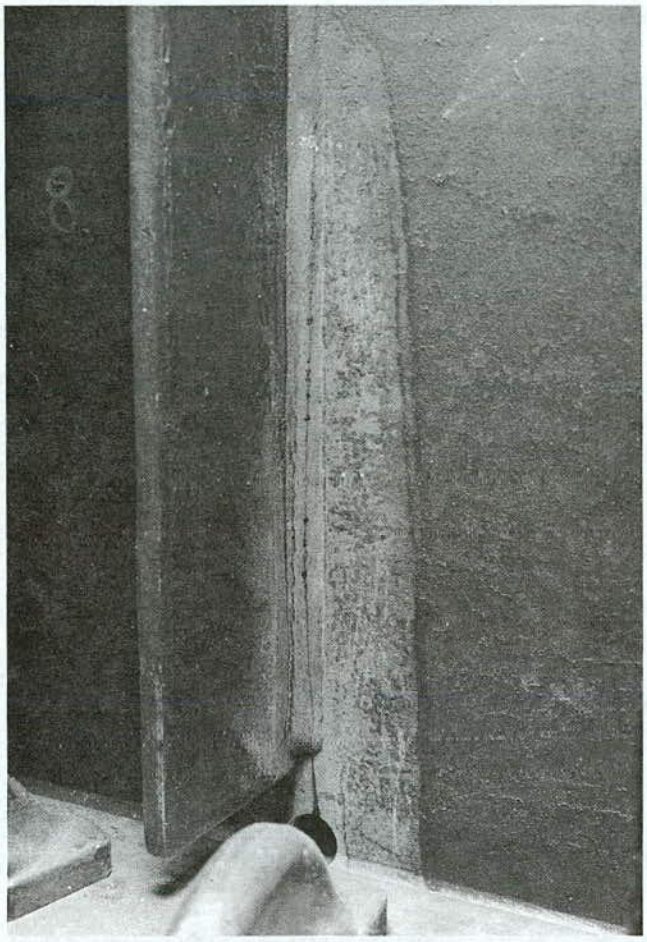

Figure 24. Fatigue crack originating on far side stiffener weld toe of Girder 2N.

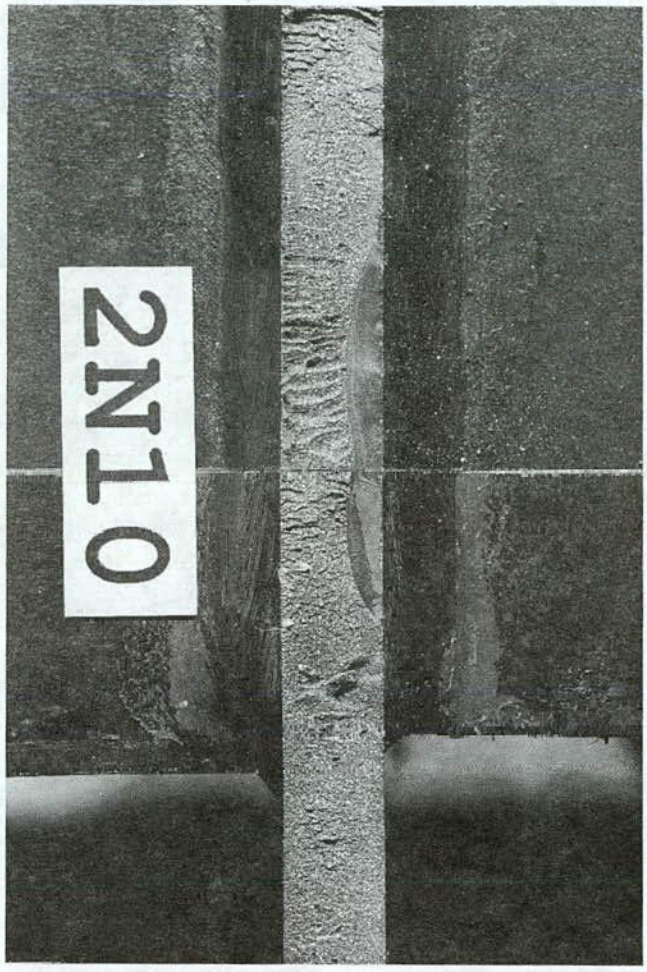

Figure 25. Fatigue crack at detail 10, Girder 2N.

At approximately 1 million random variable load cycles, the web gap cracking was retrofitted by means of drilled holes at the crack tips. Figure 30 shows the progression of fatigue cracking in stages at one of the web gap details. One and one-half-in. diameter holes were used to core out the cracking at the connection plate end, and $^3/_4$-in. diameter drilled holes were used at the tips of the web-to-flange cracks (Stage I). Within 500,000 cycles, crack reinitiation occurred at the toe of both the connection plate weld and the web-to-flange weld. The crack tips were again arrested by drilling holes, as shown in Figure 31 and testing resumed (Stage II). At 2.1×10^{-6} cycles (Stage III) and again at 2.9×10^6 cycles (Stage IV) a crack reinitiated at the drilled hole along the stiffener fillet weld toe.

At this point in the test, the diaphragms were permanently removed from the test girders to prevent further fatigue damage and avoid the possible loss of the girders due to fracture at the connection plate detail. Strain measurements taken at the top of the uppermost hole (at Stage IV) indicated that the in-plane web stresses were elevated 10 percent because of the presence of the web cracks (which reduced the section). Subsequently, a crack reinitiated at the perimeter of the drilled hole at 9.4×10^6 cycles (Stage V). The test was run an additional 20 million cycles before a toe crack reinitiated at the top hole (Stage VI). The crack tip was drilled out, and the toe of the vertical fillet welded was peened to help prevent additional cracking. At 47×10^6 cycles (Stage VII), fatigue cracks initiated at the perimeter of the uppermost hole and at one of the web-to-flange holes. The second crack represented a situation that would eventually jeopardize the test. Strain measurements on the flange plate gave an increase of 12 percent over the nominal stress based on the gross section. The crack front was drilled on both sides of the web plate and the flange plate clamped to help reduce the level of stress in the flange, minimizing the probability of continued cracking.

Retrofitting web gap cracking when it is induced by high levels of out-of-plane deformation is difficult (*6*). Even though holes were drilled at the crack tips, the level of stress from the out-of-plane motion of the diaphragm remained at such an elevated state that cracks quickly reinitiated. When the diaphragms were removed and the in-plane loading continued, the detail had previously sustained such a large magnitude of damage that cracks continued to develop and propagate. Eventually, the web cracks caused the stresses in both the web and flange plates to increase enough to initiate cracking at the perimeter of the holes. Peening stopped the crack from initiating at the weld toe.

Out-of-plane distortion on the second pair of girders was not introduced until after 100 million variable load cycles. At that time, distortion was introduced with a softer more controllable system, as illustrated in Figure 32. The web gap in Girder Pair 2 was increased to $4^1/_2$ in. (100 mm).

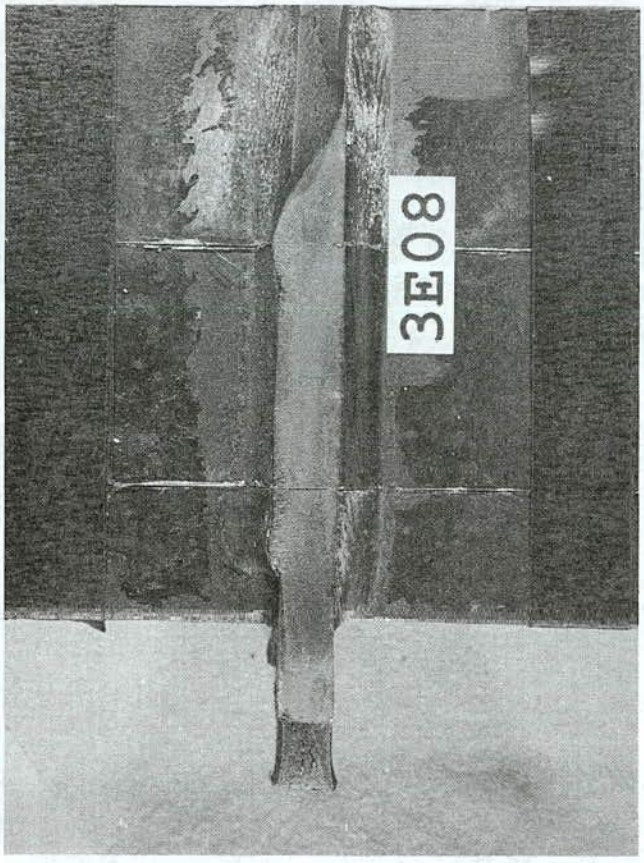

Figure 26. Crack surface at detail 3E08.

After an additional 20 million variable load cycles, small cracks were detected destructively at both transverse connection plates. Figure 33 shows the small crack that formed at detail 2N09.

EXPERIMENTAL RESULTS OF COVER-PLATED GIRDER FLANGES

The shear spans of each test girder provided Category E′ cover plate details. The applied stresses were based on the strain gage measurements and bending theory. Table 1 provides a summary of the stress range conditions at the cover plates identified as details 1 and 17. Appendix A provides greater detail on the individual stress cycles.

Girder Pair 1 was provided with end-welded cover plates and was subjected to the lowest stress cycles. Girder Pair 3 had end-welded details on one end (detail 1) and no end welds on the other end (detail 17). As can be seen from the test data summary provided in Tables 2 and 3, no fatigue cracks formed at the weld toe of any test girder cover plate with end welds.

Fatigue cracks formed at all the cover plate details on Girder Pairs 2 and 4 with the longer cover plates. Only one crack formed on Girder Pairs 1 and 3 at detail 3W17, which was a short cover plate with no end welds and with its effective stress range below the constant amplitude fatigue limit.

It was also noted that several of the cover plate details with no end welds had one or both longitudinal weld ends ground. Figure 34 compares the two types of weld ends. The ground end welds did not prevent cracks from developing at the weld termination, but did appear to slightly increase the fatigue life.

Fatigue Behavior of Cover-Plated Details

The cover-plated beam details were subjected to variable stress cycles above the Category E′ fatigue limit by frequencies between 0.3 to 100 percent (see Table 1). No fatigue cracks developed in the end-welded details on Girder Pair 1 and on Girder Pair 3 (detail 1). The exceedance frequency varied from 0.3 to 6.4 percent on these details. Table 3 shows the total cycles each of these girders was subjected to. At the details with no end welds, cracks developed when the exceedance varied from 4.3 percent to 100 percent. The final crack dimensions are given in Appendix B.

Figure 35 shows the crack that formed at detail 2N01 after 120 million variable load cycles. It can be seen that a semielliptical surface crack developed at the weld end and nearly propagated through the flange thickness. Figures 36 and 37 show two other fatigue crack surfaces: one with an as-welded detail 4E17 and one with a ground weld end (detail 4W17). Both of these details were subjected to 34.7 million variable load cycles. It is apparent

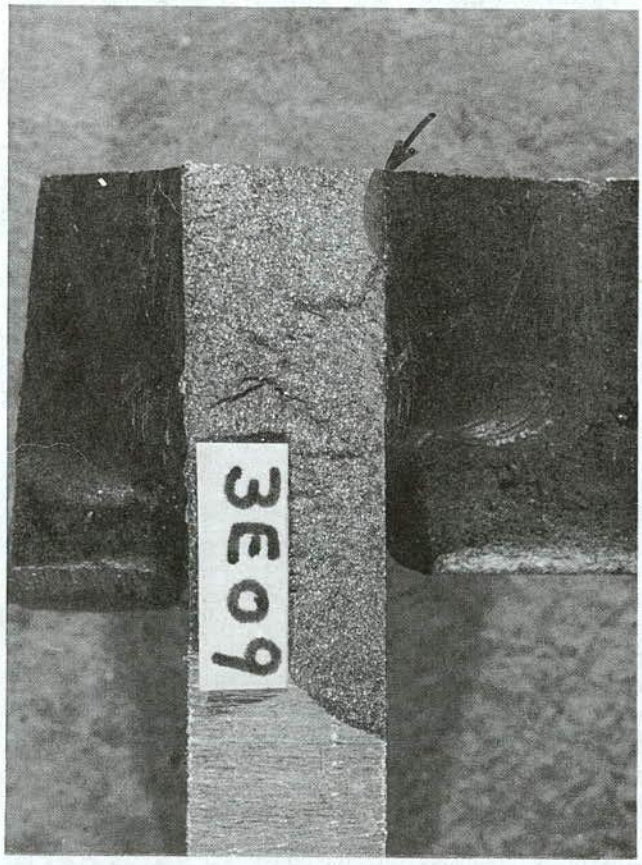

Figure 27. Small fatigue crack at detail 3E09.

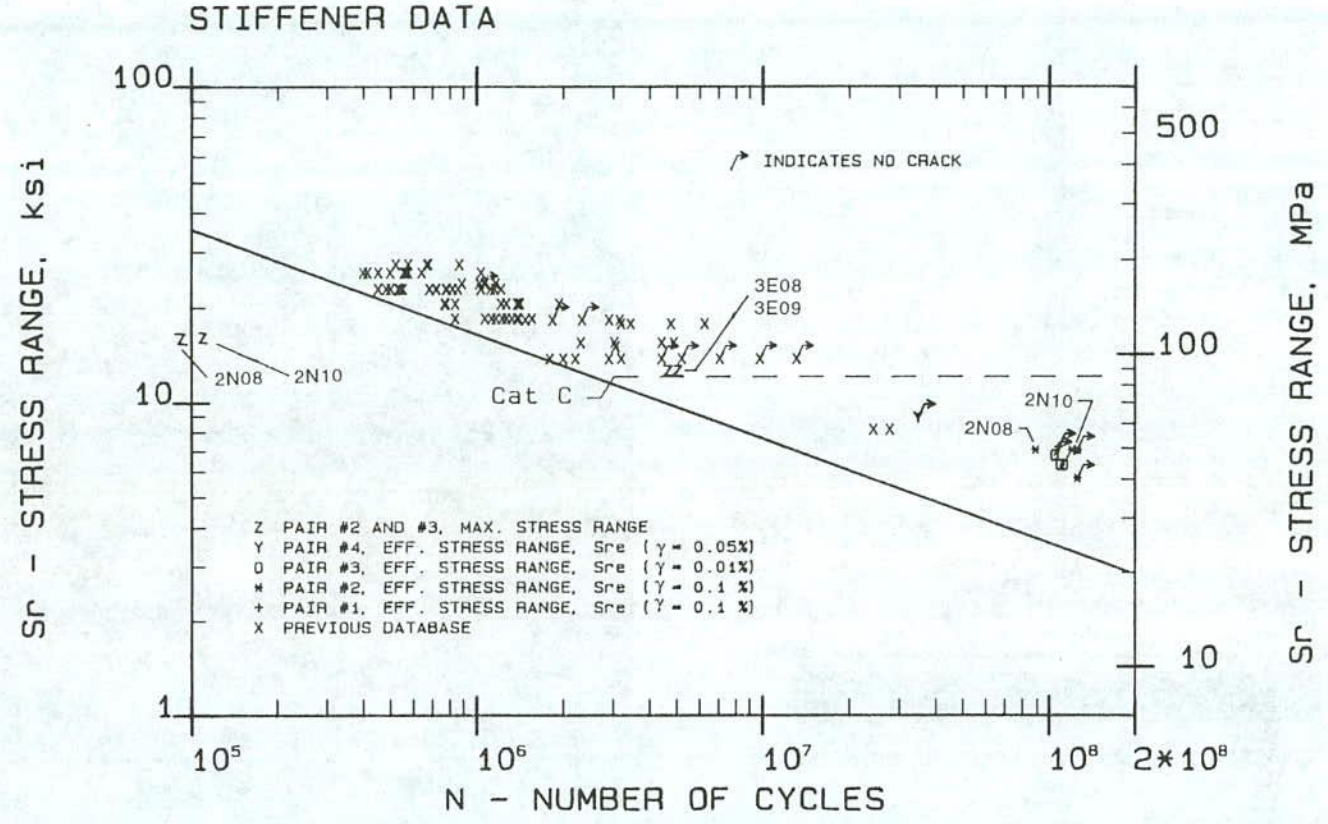

Figure 28. Comparison of test data with fatigue resistance curve for Category C.

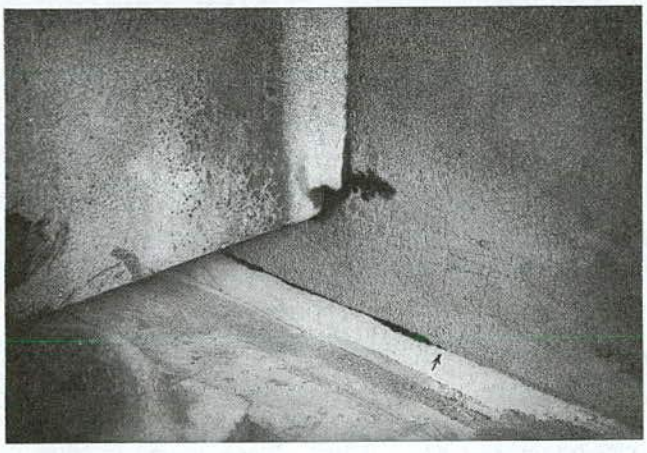

Figure 29. Fatigue cracks at web gap of 1N09

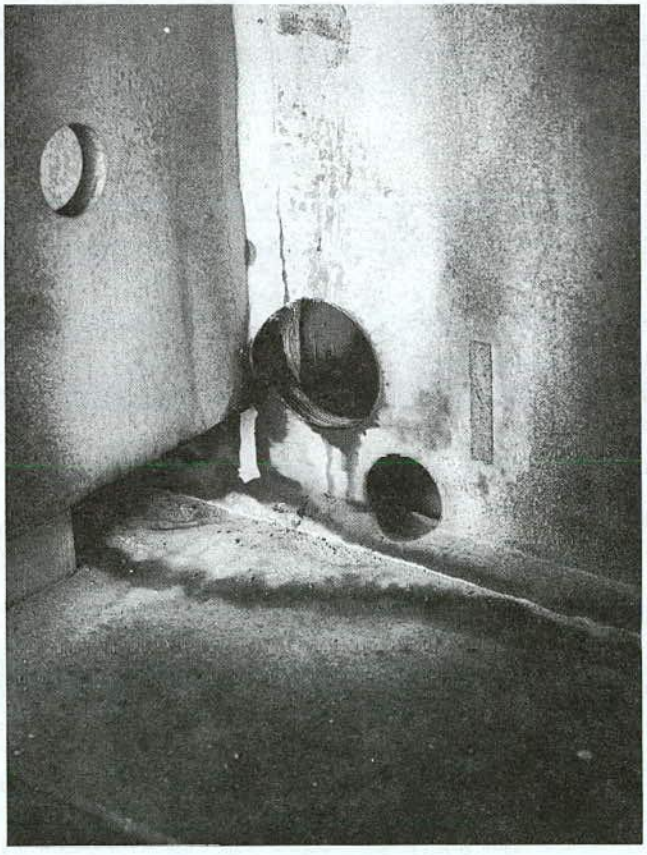

Figure 30. (Right) Retrofitted distortion cracks at detail 1N09.

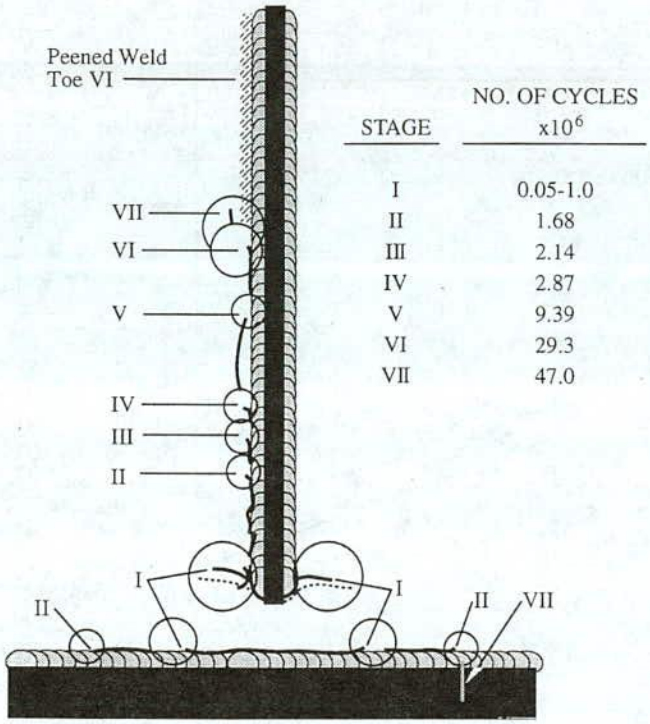

STAGE	NO. OF CYCLES x10^6
I	0.05-1.0
II	1.68
III	2.14
IV	2.87
V	9.39
VI	29.3
VII	47.0

Figure 31. Schematic history of web gap fatigue cracking.

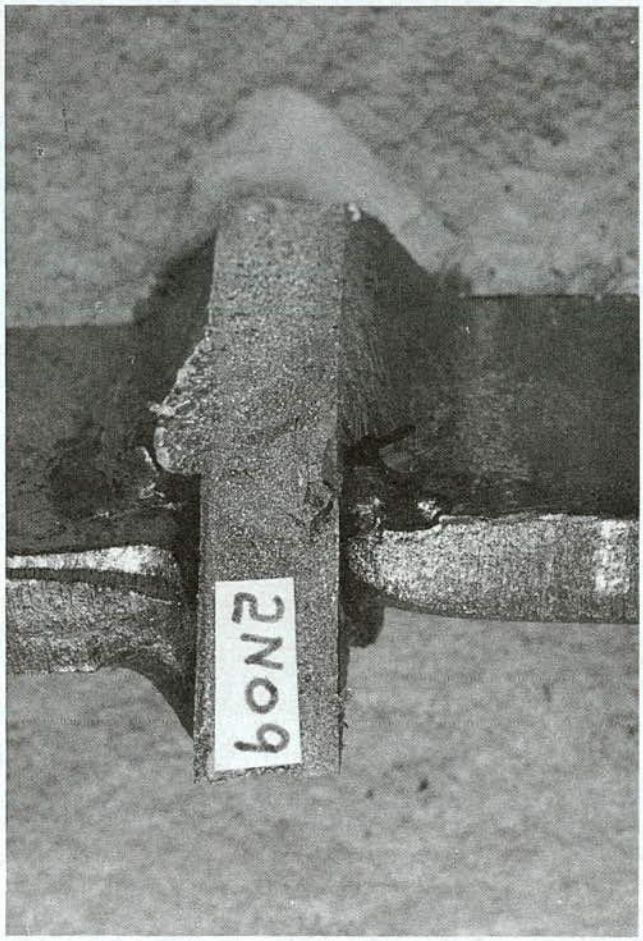

Figure 33. Small crack in Girder 2N web after distortion-induced stresses.

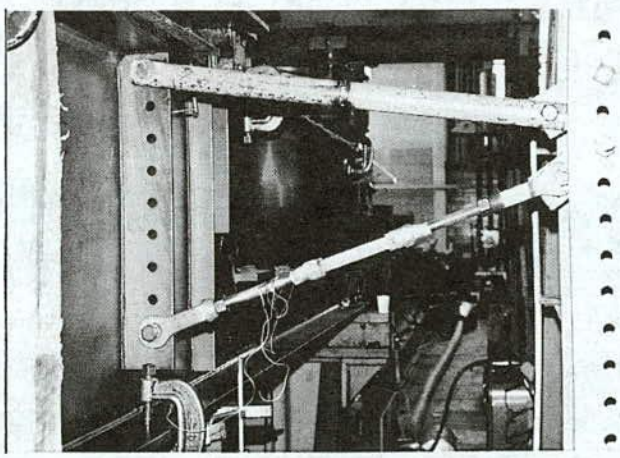

Figure 32. Web gap distortion for Girder Pair 2.

that the as-welded detail experienced more crack extension than the ground weld end.

The test results for the end-welded details are summarized in Figure 38. None of the test beams from Pairs 1 and 3 with end welds (six details) developed detectable cracks during this study. The test results from Reference 2 on Category E details with an exceedance frequency between 0.1 percent and 10.2 percent fall below or near an extension of the Category E fatigue-resistance curve. This was true for effective stress range levels above as well as below the constant amplitude fatigue limit for Category E.

The test results for the cover plate details without end welds are plotted in Figure 39. Nine of the 10 details developed fatigue cracks during the course of the variable loading (Beams 2, 4, and 3W). Fatigue cracks developed at exceedance frequencies between 4.3 and 100 percent for Category E′. The test results show that cracks were first detected near the Category E fatigue resistance curve. This was true for effective stress range values below and above the constant cycle fatigue limit for Category E′.

Hence, the full-size cover-plated beams without end welds at the cover plate termination provide a lower bound fatigue resistance similar to the web attachment details. A straight line extension of the fatigue-resistance curve below the constant cycle fatigue limit provides a lower bound to the fatigue data.

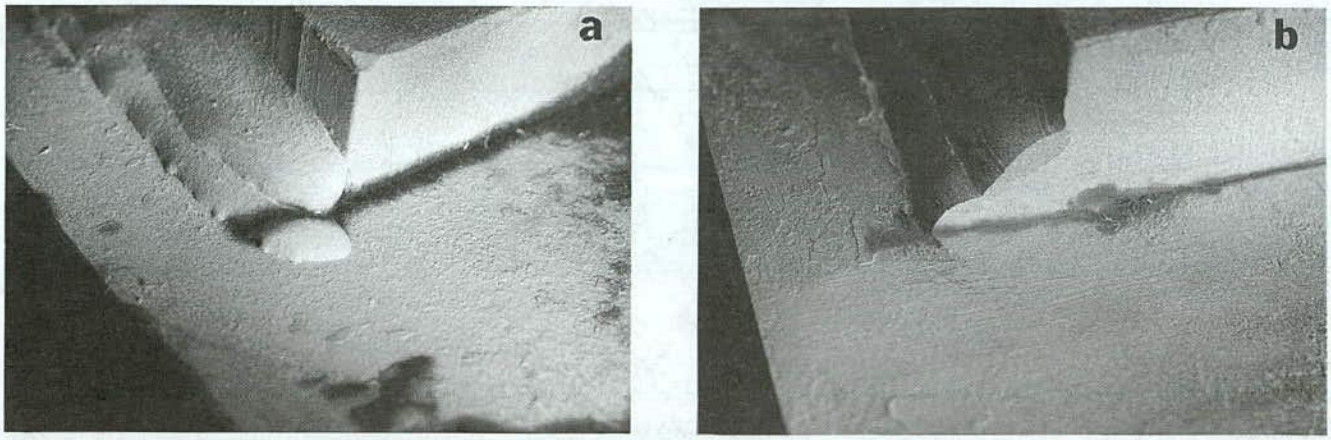

Figure 34. Typical cover plate weld terminations. (a) As-welded cover plate weld termination at detail 4E17. (b) Ground cover plate weld termination at detail 4W17.

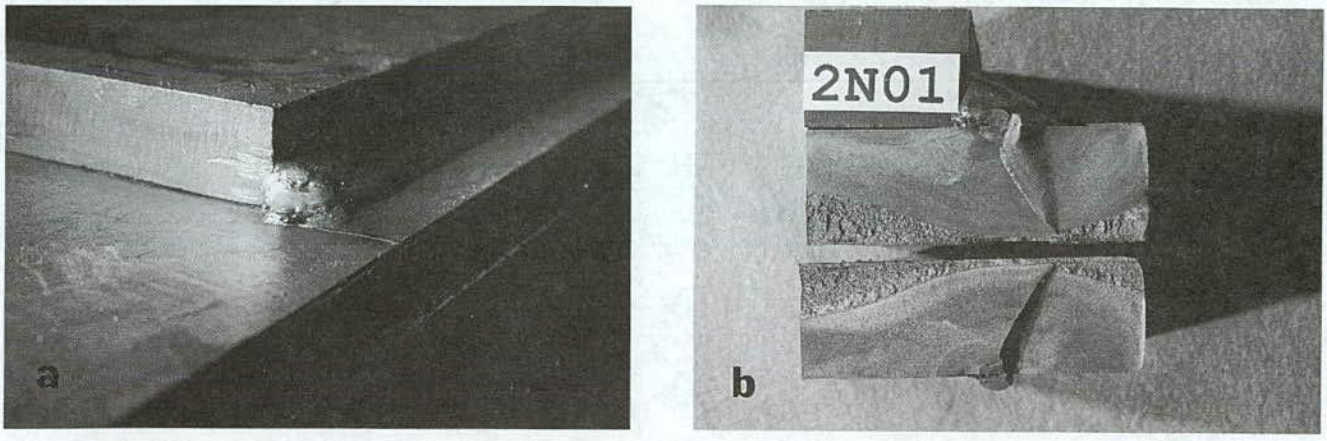

Figure 35. Fatigue crack at detail 2N01 at end of test. (a) Fatigue crack at weld termination. (b) Fatigue crack surface.

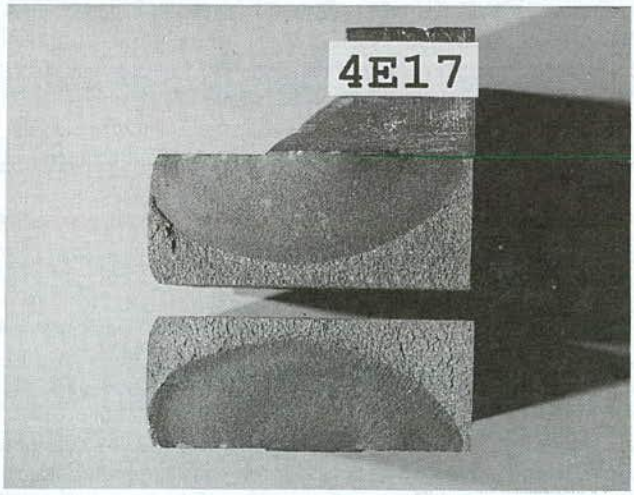

Figure 36. Fatigue crack at cover plate end weld detail 4E17.

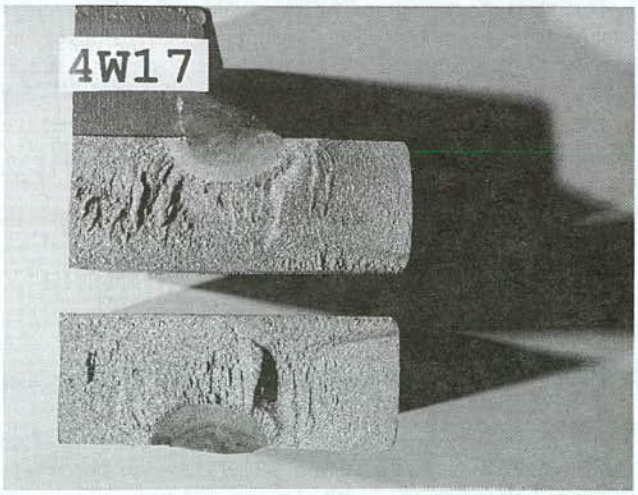

Figure 37. Fatigue crack at ground weld end detail 4W17.

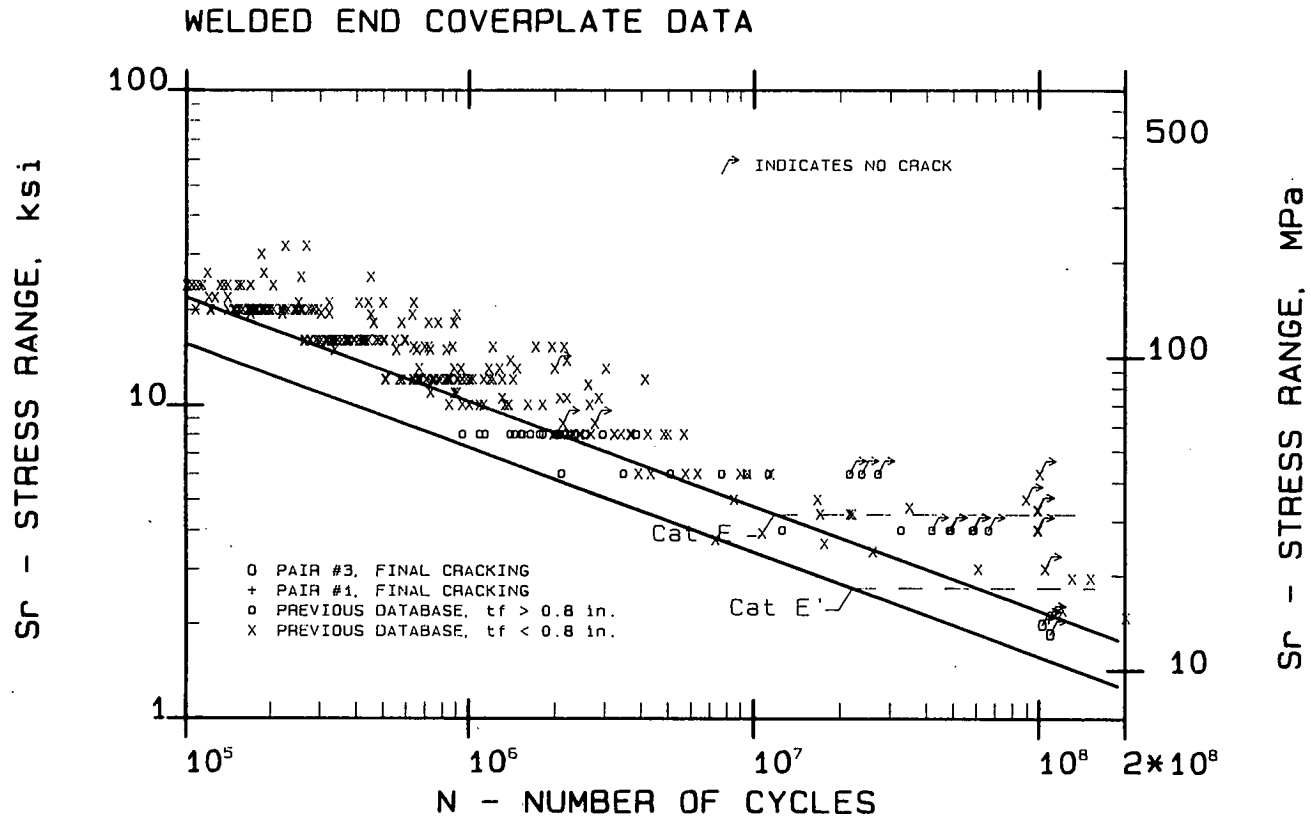

Figure 38. Comparison of the test data on end-welded cover plates with Category E and E' fatigue resistance curves.

APPLICATION OF RESULTS

The findings from this study should be of value to structural engineers involved in the design and damage assessment of welded steel members, researchers working in the subject area, and members of specification-writing organizations. The findings support the conservative design assumption that a straight-line extension of the fatigue-resistance curves for Category E and E' details, largely developed from constant amplitude loading, can be used to predict the fatigue life of details subjected to variable life loading. The experimental work of this study augments the studies reported in *NCHRP Report 267* and supports the field experience in bridge structures with Category E' details.

Fatigue Behavior of Web Gusset Plates

The study on welded web gusset plates demonstrated that fatigue cracking developed when the exceedance was greater than 0.05 percent above the constant cycle fatigue limit. This study extended the test data from *NCHRP Report 267* where the cumulative frequency exceedance for Category E' details exceeded 13.9 percent.

These tests further support the hypothesis that stress cycles below the constant cycle fatigue limit will contribute to crack growth more than that predicted from modeling. Cracking developed when the effective stress range was below the constant cycle fatigue limit. The study also confirmed that care must be exercised at weld toe terminations to ensure that large initial defects (undercuts, gouges, etc.) do not reside at the weld toe. This resulted in premature cracking at a low effective stress range and a significant reduction in fatigue life.

Grinding the weld end did not have a significant effect on the test results as few of the details had the end weld termination ground on each side of the web.

Fatigue Behavior of Stiffeners

Of the 20 stiffener details not subjected to out-of-plane distortion, only four developed fatigue cracks in this study. Two of these cracks could be accounted for by considering only the maximum stress range in the variable spectrum (3E08, 3E09). They correlated with the fatigue resistance provided by constant cycle data, and stress cycles below the constant cycle fatigue limit did not appear to contribute to the fatigue damage. However, two other details (2N08, 2N10) subjected to only 89,500 and

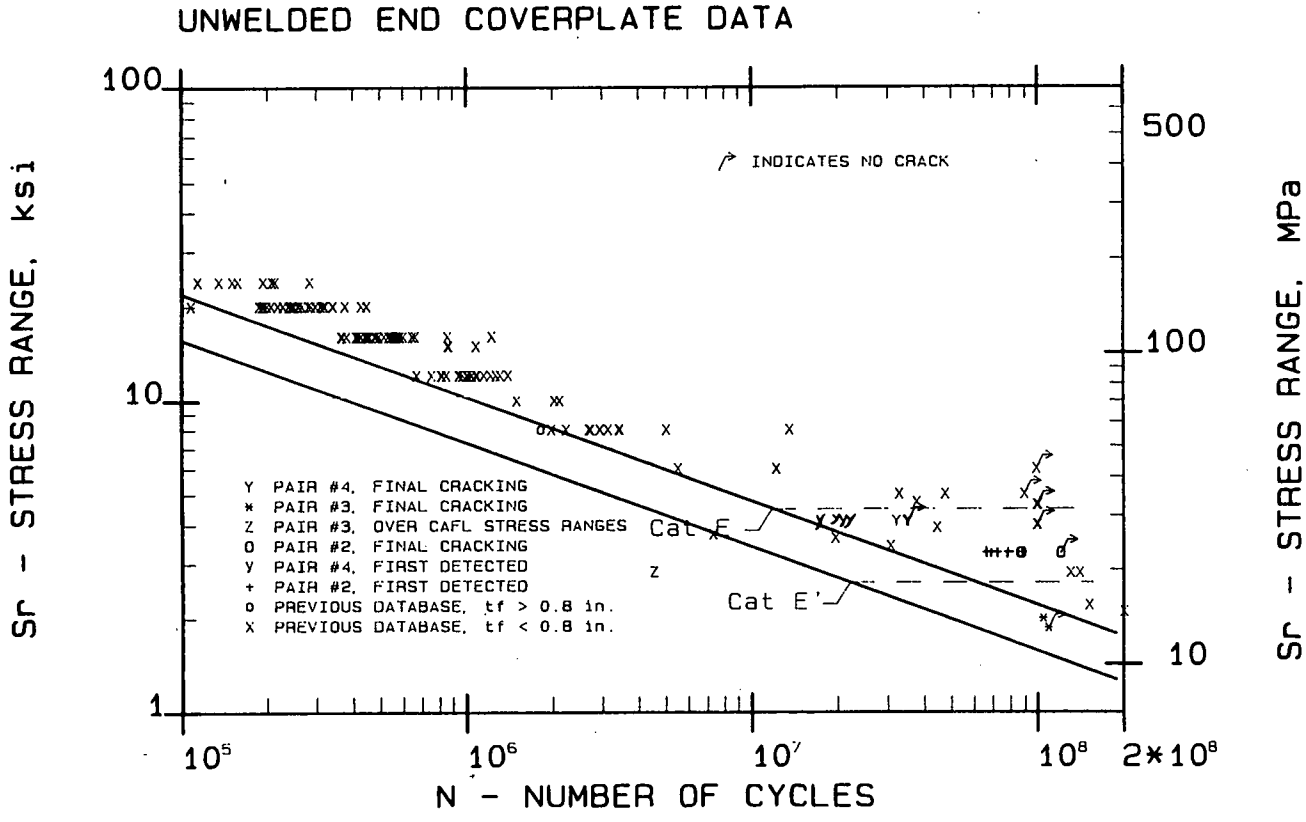

Figure 39. Comparison of the test data on cover plate details without end welds with Category E and E' fatigue resistance curves.

120,000 cycles above the constant cycle fatigue limit developed fatigue cracks. These details could only be correlated with the fatigue-resistance curve when all cycles in the variable load spectrum were considered. The test data with effective stress range below the constant cycle fatigue limit all plotted well beyond the extension of the Category C fatigue-resistance curve.

The test results suggest that fatigue cracks are not likely to develop at transverse stiffener details in actual bridge structures unless out-of-plane distortion develops.

The studies on out-of-plane distortion of transverse connection plates confirmed the findings given in *NCHRP Report 336*. Rigid connections of the plate to the top and bottom flanges by bolted or welded connections are needed to prevent fatigue cracks from out-of-plane deformation.

Fatigue Behavior of Cover Plates

The test results on Category E' cover-plated beams ($t_f > 0.8$ in.) provided behavior similar to the results reported in *NCHRP Report 267* on Category E cover plate details. Variable stress spectrums with cumulative exceedance frequencies greater than 4.3 percent resulted in fatigue cracks when the effective stress range was below the constant cycle fatigue limit.

No cracks were detected at cover-plated details with transverse end welds when the cumulative exceedance was below 6.4 percent. In those tests the maximum stress range was between 3.7 ksi (25.5 MPa) and 4.4 ksi (30 MPa). The girder subjected to 3.7 ksi (25.5 MPa) was subjected to just over 5×10^6 cycles at that stress range.

CHAPTER 4

CONCLUSIONS AND SUGGESTED RESEARCH

The conclusions in this chapter are based on an analysis and evaluation of the test data acquired during this experimental study, and on the results of other experimental studies on large-scale specimens.

FATIGUE BEHAVIOR OF WEB GUSSET PLATES

This experimental study provided test results compatible with the results reported in *NCHRP Report 267*. Category E′ was verified to be the applicable fatigue-resistance curve. These tests demonstrated that low levels of exceedance of the constant amplitude fatigue limit (CAFL) resulted in fatigue cracking even when the effective stress range was below the CAFL. The current practice of using a straight-line extension of the sloping portion of the constant amplitude S-N curve to determine fatigue life should be retained.

A small gouge or undercut at the weld toe was found to significantly reduce the fatigue resistance of the web gusset plate detail. Cracking developed below the Category E′ fatigue resistance curve when this type of defect was present.

FATIGUE BEHAVIOR OF TRANSVERSE STIFFENERS

The tests on transverse stiffeners and connection plates demonstrated that the stiffener details were not as susceptible to fatigue cracking at low levels of exceedance (0.01 to 0.1 percent) when the peak stress range was less than 16 ksi. When cracks did develop, the test data were found to plot well beyond the straight-line extension of the Category C fatigue-resistance curve. Cracks also developed in Girder 3E subjected to 5×10^6 cycles of constant cycle loading at the peak stress range of 12.5 ksi (86 MPa), which is just slightly above the estimated CAFL. This verified the applicability of the constant amplitude fatigue limit for stiffener details.

The test results suggest that stiffener details are not likely to develop fatigue cracks in service. Available field test data indicate that the constant amplitude fatigue limit will not be exceeded enough to cause significant fatigue damage to in-service structures.

The girders with transverse connecting plates subjected to out-of-plane distortion provided test results that were compatible with the findings presented in *NCHRP Report 336*. Small web gaps were found to be very susceptible to fatigue cracking. An increased gap length of 4½ in. (100 mm) reduced the sensitivity to fatigue cracking for moderate levels of out-of-plane movement.

FATIGUE BEHAVIOR OF COVER PLATE DETAILS

The limited data on large-scale cover-plated beams corresponding to Category E′ demonstrated that fatigue cracks formed at cover plates without transverse end welds when the constant amplitude fatigue limit (CAFL) was exceeded by 4.3 percent or more of the variable amplitude cycles. The effective stress range was below the CAFL for this load spectrum.

Therefore, for fatigue analysis of details subjected to variable amplitude loading, all stress cycles above 50 percent of the constant amplitude fatigue limit for the appropriate detail should be considered to cause fatigue damage.

This observation is based on the analytical studies summarized in Chapter 3, as well as experience with actual bridge structures. An example can be seen from the stress range spectrum shown in Figure 8 and the corresponding analytical results plotted in Figure 9b.

RETROFITTING WEB CRACKS

The variable amplitude loading verified the adequacy of arresting fatigue crack extension in girder webs by holes placed at the tips of the cracks. Fatigue cracks were arrested when the following relationship was satisfied:

$$\frac{\Delta K_{max}}{\sqrt{\rho}} < 4\sqrt{\sigma_y} \text{ (for } \sigma_y \text{ in ksi)}$$

$$\frac{\Delta K_{max}}{\sqrt{\rho}} < 10.5\sqrt{\sigma_y} \text{ (for } \sigma_y \text{ in MPa)}$$

ΔK_{max} was defined by the largest stress cycle in the variable load spectrum.

The equation above can be put into a more usable form by letting L be equal to the total length of the retrofitted crack $2a$ (see Figure 21) and ϕ equal to the hole diameter 2ρ. With appropriate substitutions for ΔK a minimum hole diameter can be expressed as:

$$\phi \geq \frac{S_r^2 L}{5\sigma_y} \text{ (for } \sigma_y \text{ in ksi)} \quad (7a)$$

$$\phi \geq \frac{S_r^2 L}{35\sigma_y} \text{ (for } \sigma_y \text{ in MPa)} \quad (7b)$$

Strain measurements of in-service bridges have indicated that the stress range seldom exceeds 6.0 ksi (41 MPa). Therefore, for plates having yield stress of 36 ksi (248 MPa), a diameter between $\frac{3}{4}$ in. (19 mm) and 1.0 in. (25 mm) is usually sufficient.

A factor not considered in the development of Equation (6) was the method of hole preparation and degree of finish given to the hole. If burrs or rough edges remain after the drilling operation, crack initiation may occur because of the stress risers. All drilled holes should be ground to a polished finish. Dye penetrant inspection should be performed on completion to ensure that the hole circumference is free of defects and that the crack tip has been properly located and removed.

Only limited data were obtained on the transverse connection plate details. Large out-of-plane deformation that resulted in fatigue cracks in girder webs made the cracks difficult to arrest. It was necessary to minimize the out-of-plane deformation before the cracks could be arrested.

RECOMMENDATIONS FOR FURTHER RESEARCH

1. The laboratory fatigue tests provided in this report, other tests available from prior studies, and other current ongoing work indicate that additional tests are desirable under extreme life conditions. The data on stiffener details remain sparse in the high-cycle region. The indication is that Category C details (stiffeners and transverse connection plates) will not be susceptible to fatigue damage in actual bridge structures if out-of-plane distortions are limited. Additional experimental data would help to solidify the validity of this common detail condition.
2. Variable load tests are needed on riveted bridge members. No significant variable load data are available on the class of joint. Existing experimental data have demonstrated that Category C is a good estimate of fatigue strength for riveted details. Variable cycle data on this detail would provide damage criteria for use on many thousands of older bridge structures.
3. Variable load tests are needed on Category D welded details in the extreme life region. The limited number of tests on this class of detail is insufficient to properly assess its fatigue behavior in this region of fatigue life.

REFERENCES

1. Fisher, J.W., *Fatigue and Fracture of Steel Bridges—Case Studies,* John Wiley and Sons (1984).
2. Fisher, J.W., Mertz, D.R., and Zhong, A., "Steel Bridge Members Under Variable Amplitude Long Life Fatigue Loading," *NCHRP Report 267,* Transportation Research Board, Washington, D.C. (1983).
3. Schilling, C.G., Klippstein, K.H., Barsom, J.M., and Blake, G.T., "Fatigue of Welded Steel Bridge Members Under Variable-Amplitude Loading," *NCHRP Report 188,* Transportation Research Board, Washington, D.C. (1978).
4. Albrecht, P. and Friedland, I.M., "Fatigue Limit Effect on Variable-Amplitude Fatigue of Stiffeners," *J. Struct. Eng.,* ASCE, Vol. 105 (ST12) (Dec. 1979), pp. 2657–2675.
5. Keating, P.B. and Fisher, J.W., "Evaluation of Fatigue Tests and Design Criteria on Welded Details," *NCHRP Report 286,* Transportation Research Board, Washington, D.C. (Sept. 1986).
6. Albrecht, P.A. and Rubeiz, C.G., "Variable Amplitude Fatigue Behavior—Task A—Literature Review," Pub. No. *FHWA-RD-87-061* (July 1990).
7. Fisher, J.W., Jian, J., Wagner, D.C. and Yen, B.T., "Distortion-Induced Fatigue Cracking in Steel Bridges," *NCHRP Report 336,* Transportation Research Board, Washington, D.C. (Dec. 1990).
8. Tada, H., Paris, P.C., and Irwin, G.R., *The Stress Analysis of Cracks Handbook,* Del Research Corp., Hellertown, PA (1973).
9. Maddox, S.J., "Assessing the Significance of Flaws in Welds Subject to Fatigue," *Welding J.,* Vol. 53 (Sept. 1974).
10. Albrecht, P. and Yamada, K., "Rapid Calculation of Stress Intensity Factors," *J. Struct. Engin.,* ASCE, Vol. 103 (ST2) (Feb. 1977).
11. Zettlemoyer, N. and Fisher, J.W., "Stress Gradient Correction Factors for Stress Intensity at Welded Stiffeners and Cover Plates," *Welding Research Supplement,* AWS, Vol. 12 (Dec. 1977), pp. 393s–397s.
12. Norris, S.N. and Fisher, J.W., "The Fatigue Behavior of Welded Web Attachments," *J. Construct. Steel Research,* No. 2 (Jan. 1981).
13. Fisher, J.W., Hausammann, H., Sullivan, M.D., and Pense, A.W., "Detection and Repair of Fatigue Damage in Welded Highway Bridges," *NCHRP Report 206,* Transportation Research Board (1979).
14. Fisher, J.W., Barthelemy, B.M., Mertz, D.R., and Edinger, J.A., "Fatigue Behavior of Full-Scale Welded Bridge Attachments," *NCHRP Report 227,* Transportation Research Board (1980).
15. "Fatigue Phenomena in Welded Connections of Bridges and Cranes," *ORE Report D 130,* Office of Research and Experiments of the International Union of Railways, Reports D130/RP 1/E through D130/RP 10/E (1974–1979).

APPENDIX A

FREQUENCY AND STRESS RANGE DATA FOR TEST BEAMS

Appendix A provides details of the stress range levels and their frequency of occurrence for each test girder detail. The first column of each Table provides the jack load level as a percent of the maximum cyclic load in the variable load spectrum. The stress range corresponding to the cyclic load for each detail is tabulated in ksi. The bold underline indicates the boundary between stress cycles below and above the constant cycle fatigue limit used in the specifications. The last column shows the frequency of occurrence, α, of the stress cycles.

Table A1: Stress Ranges for Details of Girder Pair 1

STRESS RANGE S_{ri}, FOR DETAILS (ksi)

Type	Cover Plate	Web Attachment						Stiff.	Freq. α_i
Detail No. / Load Level	1 & 17	2 & 16	3 & 15	4 & 14	5 & 13	6 & 12	7 & 11	8 9 10	α
31.2%	1.30	0.85	1.08	1.10	1.29	1.34	1.51	4.37	0.073
37.6%	1.56	1.02	1.30	1.32	1.55	1.61	1.82	5.26	0.19
43.4%	1.80	1.18	1.51	1.53	1.80	1.86	2.10	6.08	0.237
49.5%	2.05	1.34	1.72	1.74	2.05	2.12	2.40	6.93	0.207
55.6%	2.31	1.51	1.93	1.95	2.30	2.38	2.69	7.78	0.146
61.7%	2.56	1.67	2.14	2.17	2.55	2.65	2.99	8.64	0.083
67.8%	2.81	1.84	2.35	2.38	2.81	2.91	3.28	9.49	0.04
73.6%	3.05	2.00	2.55	2.59	3.05	3.16	3.57	10.31	0.016
79.7%	3.31	2.16	2.76	2.81	3.30	3.42	3.86	11.16	0.005
85.7%	3.56	2.32	2.97	3.02	3.55	3.68	4.15	12.0	0.002
100%	4.15	2.71	3.47	3.52	4.14	4.29	4.84	14.0	0.001
S_{re} (RMC)	2.07	1.36	1.74	1.76	2.08	2.15	2.42	7.02	

Table A2: Stress Ranges for Details of Girder Pair 2

STRESS RANGE S_{ri}, FOR DETAILS (ksi)

Type	Cover Plate	Web Attachment							Stiff.	Freq. α_i
Load Level \ Detail No.	1 & 17	2 & 16	3 & 15	4 & 14	5 & 13	6 & 12	7 & 11	8 & 10	9	α
24.3%	2.03	0.85	1.08	1.10	1.29	1.34	1.51	4.37	3.53	0.073
29.2%	2.44	1.02	1.30	1.32	1.55	1.61	1.82	5.26	4.24	0.19
33.8%	2.82	1.18	1.51	1.53	1.80	1.86	2.10	6.08	4.91	0.237
38.5%	3.21	1.34	1.72	1.74	2.05	2.12	2.40	6.93	5.59	0.207
43.2%	3.60	1.51	1.93	1.95	2.30	2.38	2.69	7.78	6.27	0.146
48.0%	4.00	1.67	2.14	2.17	2.55	2.65	2.99	8.64	6.97	0.083
52.7%	4.39	1.84	2.35	2.38	2.81	2.91	3.28	9.49	7.65	0.04
57.3%	4.78	2.00	2.55	2.59	3.05	3.16	3.57	10.31	8.32	0.016
62.0%	5.17	2.16	2.76	2.81	3.30	3.42	3.86	11.16	9.00	0.005
66.7%	5.56	2.32	2.97	3.02	3.55	3.68	4.15	12.0	9.68	0.002
100%	8.34	3.49	4.46	4.52	5.32	5.51	6.22	18.0	14.52	0.001
S_{re} (RMC)	3.25	1.36	1.74	1.76	2.08	2.15	2.42	7.02	5.66	

Table A3: Stress Ranges for Details of Girder 3W

STRESS RANGE S_{ri}, FOR DETAILS (ksi)

Type	Cover Plate	Web Attachment							Stiff.	Freq. α_i
Load Level \ Detail No.	1 & 17	2 & 16	3 & 15	4 & 14	5 & 13	6 & 12	7 & 11	8 9 10		α
31.3%	1.38	0.91	1.16	1.18	1.38	1.43	1.62	4.69		0.017
34.4%	1.53	1.00	1.28	1.29	1.53	1.58	1.78	5.16		0.12
37.5%	1.67	1.09	1.40	1.42	1.66	1.73	1.94	5.63		0.17
40.6%	1.81	1.18	1.51	1.53	1.80	1.87	2.11	6.09		0.19
43.8%	1.95	1.28	1.63	1.65	1.94	2.02	2.27	6.56		0.16
46.9%	2.08	1.36	1.74	1.77	2.08	2.16	2.43	7.03		0.13
50.0%	2.22	1.45	1.86	1.88	2.22	2.30	2.60	7.50		0.08
53.1%	2.36	1.54	1.97	2.00	2.35	2.44	2.76	7.97		0.06
56.3%	2.50	1.63	2.09	2.12	2.49	2.59	2.92	8.44		0.03
59.4%	2.64	1.73	2.20	2.24	2.63	2.73	3.08	8.90		0.02
62.5%	2.77	1.82	2.33	2.35	2.78	2.87	3.24	9.38		0.01
65.6%	2.92	1.90	2.44	2.48	2.91	3.00	3.40	9.84		0.006
68.8%	3.06	2.00	2.56	2.60	3.06	3.16	3.57	10.31		0.004
71.9%	3.20	2.09	2.67	2.71	3.19	3.30	3.73	10.78		0.002
75.0%	3.34	2.18	2.78	2.83	3.33	3.45	3.89	11.25		0.001
100%	4.44	2.90	3.71	3.77	4.43	4.59	5.18	15.00		0.0001
S_{re} (RMC)	1.99	1.29	1.66	1.69	1.98	2.05	2.31	6.70		

Table A4: Stress Ranges for Details of Girder 3E

STRESS RANGE S_{ri}, FOR DETAILS (ksi)

Type	Cover Plate	Web Attachment						Stiff.	Freq. α_i
Detail No. / Load Level	1 & 17	2 & 16	3 & 15	4 & 14	5 & 13	6 & 12	7 & 11	8 9 10	α
31.3%	1.16	0.76	0.97	0.98	1.16	1.20	1.35	3.91	0.017
34.4%	1.27	0.84	1.06	1.08	1.27	1.32	1.48	4.30	0.12
37.5%	1.39	0.91	1.16	1.18	1.38	1.44	1.62	4.69	0.17
40.6%	1.51	0.98	1.26	1.27	1.50	1.55	1.76	5.08	0.19
43.8%	1.63	1.06	1.36	1.38	1.62	1.68	1.89	5.47	0.16
46.9%	1.73	1.13	1.45	1.48	1.73	1.80	2.02	5.86	0.13
50.0%	1.85	1.21	1.55	1.57	1.85	1.91	2.16	6.25	0.08
53.1%	1.97	1.28	1.64	1.67	1.96	2.03	2.30	6.64	0.06
56.3%	2.09	1.36	1.74	1.77	2.08	2.16	2.43	7.03	0.03
59.4%	2.20	1.44	1.84	1.87	2.20	2.27	2.57	7.42	0.02
62.5%	2.31	1.52	1.94	1.96	2.31	2.39	2.70	7.81	0.01
65.6%	2.43	1.59	2.03	2.06	2.42	2.51	2.84	8.20	0.006
68.8%	2.55	1.66	2.13	2.16	2.55	2.63	2.98	8.59	0.004
71.9%	2.66	1.74	2.23	2.26	2.66	2.75	3.11	8.98	0.002
75.0%	2.78	1.81	2.32	2.36	2.77	2.88	3.24	9.38	0.001
100%	3.70	2.42	3.09	3.14	3.70	3.83	4.32	12.5	0.0001
S_{re} (RMC)	1.66	1.08	1.38	1.41	1.65	1.71	1.93	5.59	

Table A5: Stress Ranges for Details of Girder Pair 4

STRESS RANGE S_{ri}, FOR DETAILS (ksi)

Type	Cover Plate	Web Attachment						Stiff.	Freq. α_i
Detail No. / Load Level	1 & 17	2 & 16	3 & 15	4 & 14	5 & 13	6 & 12	7 & 11	8 9 10	α
50.0%	3.71	1.55	1.98	2.01	2.37	2.45	2.77	8.0	0.335
53.1%	3.94	1.64	2.10	2.14	2.51	2.60	2.94	8.5	0.3
56.3%	4.17	1.74	2.23	2.26	2.66	2.76	3.11	9.0	0.15
59.4%	4.40	1.84	2.35	2.39	2.81	2.91	3.29	9.5	0.10
62.5%	4.63	1.94	2.48	2.51	2.96	3.06	3.46	10.0	0.05
65.6%	4.86	2.03	2.60	2.64	3.10	3.21	3.63	10.5	0.03
68.8%	5.10	2.13	2.73	2.77	3.26	3.37	3.81	11.0	0.02
71.9%	5.33	2.23	2.85	2.89	3.40	3.52	3.98	11.5	0.01
75.0%	5.56	2.32	2.97	3.02	3.55	3.68	4.15	12.0	0.005
100%	7.41	3.10	3.96	4.02	4.73	4.90	5.53	16.0	0.0005
S_{re} (RMC)	4.09	1.71	2.18	2.22	2.61	2.70	3.05	8.83	

APPENDIX B

FINAL CRACK SIZES

Appendix B provides a tabulation of the final crack sizes observed at each cracked detail. Table B1 provides the depth, α, of surface cracks or the half length of through cracks. All dimensions are provided in inches. Table B2 provides the length 2C of all the surface cracks that are not through thickness. Through-thickness cracks are designated as Th. Sketches are provided with each table to assist with the crack definition.

Table B1: Final crack sizes, depth or length a [in] at end of test or at time of retrofit

Girder		1N	1S	2N	2S	3W	3E	4W	4E
Total Cycles		107.2	107.2	120	120	104	109	34.7	34.7
Detail									
Coverplate	1	-	-	0.43	0.46	-	-	0.71	0.65
	1	-	-	2.50	0.63	-	-	-	-
	2	-	-	1.30	0.48	-	-	-	-
	3	-	1.00	-	0.35	-	-	-	-
Web	4	-	-	-	0.15	-	-	-	-
attachment	5	-	-	0.12	1.15	-	-	-	0.20
	6	-	1.50	0.15	0.16*	-	-	-	1.50
	7	-	-	2.50	1.25	1.75	1.25	-	-
Stiffener	8	-	-	4.45	-	-	2.25	-	-
	9	1.50	1.00	0.06*	0.08*	-	0.06*	-	-
	10	-	-	0.14*	-	-	-	-	-
	11	-	2.25	3.62	3.25	-	0.16*	2.50	-
	12	-	-	0.50	-	2.25	0.06*	1.25	-
Web	13	-	-	0.50	2.37	-	-	2.20	0.30
Attachment	14	-	-	-	-	-	-	0.35	-
	15	-	-	0.16	0.10	-	-	-	-
	16	-	-	0.16	0.20	-	-	-	1.75
	17	-	-	0.65	0.33	0.04*	-	0.35	0.88
Coverplate	17	-	-	-	0.35	-	-	0.28	0.34

* = Detected by destructive examination

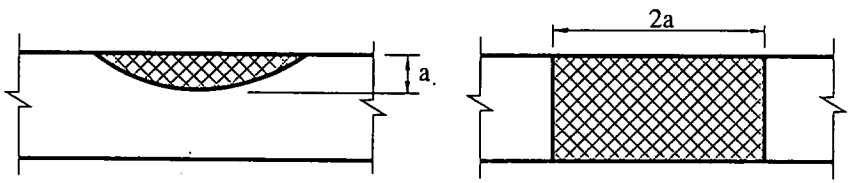

Table B2: Final crack sizes, length 2c [in] at end of test or at time of first retrofit

Girder		1N	1S	2N	2S	3W	3E	4W	4E
Total Cycles		107.2	107.2	120	120	104	109	34.7	34.7
Detail									
Coverplate	1	-	-	1.06	1.16	-	-	2.15	1.60
	1	-	-	Th.	1.75	-	-	-	-
	2	-	-	Th.	1.10	-	-	-	-
	3	-	Th.	-	1.20	-	-	-	-
Web	4	-	-	-	0.25	-	-	-	-
attachment	5	-	-	0.25	Th.	-	-	-	0.50
	6	-	Th.	0.30	0.37*	-	-	-	Th.
	7	-	-	Th.	Th.	Th.	Th.	-	-
Stiffener	8	-	-	Th.	-	-	Th.	-	-
	9	Th.	Th.	0.18*	0.20*	-	0.19*	-	-
	10	-	-	1.50*	-	-	-	-	-
	11	-	Th.	Th.	Th.	-	0.75*	Th.	-
	12	-	-	Th.	-	Th.	0.09*	Th.	-
Web	13	-	-	Th.	Th.	-	-	Th.	0.75
attachment	14	-	-	-	-	-	-	1.25	-
	15	-	-	0.40	0.20	-	-	-	-
	16	-	-	0.40	0.50	-	-	-	Th.
	17	-	-	1.70	0.73	0.12*	-	0.92	2.42
Coverplate	17	-	-	-	0.68	-	-	0.30	0.75

* = Detected by destructive examination
Th. = Through-thickness crack (see Table B1)

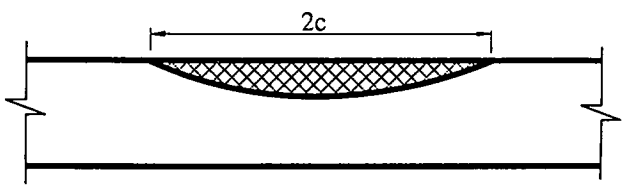

THE TRANSPORTATION RESEARCH BOARD is a unit of the National Research Council, which serves the National Academy of Sciences and the National Academy of Engineering. It evolved in 1974 from the Highway Research Board which was established in 1920. The TRB incorporates all former HRB activities and also performs additional functions under a broader scope involving all modes of transportation and the interactions of transportation with society. The Board's purpose is to stimulate research concerning the nature and performance of transportation systems, to disseminate information that the research produces, and to encourage the application of appropriate research findings. The Board's program is carried out by more than 270 committees, task forces, and panels composed of more than 3,300 administrators, engineers, social scientists, attorneys, educators, and others concerned with transportation; they serve without compensation. The program is supported by state transportation and highway departments, the modal administrations of the U.S. Department of Transportation, the Association of American Railroads, the National Highway Traffic Safety Administration, and other organizations and individuals interested in the development of transportation.

The National Academy of Sciences is a private, nonprofit, self-perpetuating society of distinguished scholars engaged in scientific and engineering research, dedicated to the furtherance of science and technology and to their use for the general welfare. Upon the authority of the charter granted to it by the Congress in 1863, the Academy has a mandate that requires it to advise the federal government on scientific and technical matters. Dr. Frank Press is president of the National Academy of Sciences.

The National Academy of Engineering was established in 1964, under the charter of the National Academy of Sciences, as a parallel organization of outstanding engineers. It is autonomous in its administration and in the selection of its members, sharing with the National Academy of Sciences the responsibility for advising the federal government. The National Academy of Engineering also sponsors engineering programs aimed at meeting national needs, encourages education and research and recognizes the superior achievements of engineers. Dr. Robert M. White is president of the National Academy of Engineering.

The Institute of Medicine was established in 1970 by the National Academy of Sciences to secure the services of eminent members of appropriate professions in the examination of policy matters pertaining to the health of the public. The Institute acts under the responsibility given to the National Academy of Sciences by its congressional charter to be an adviser to the federal government and, upon its own initiative, to identify issues of medical care, research, and education. Dr. Kenneth I. Shine is president of the Institute of Medicine.

The National Research Council was organized by the National Academy of Sciences in 1916 to associate the broad community of science and technology with the Academy's purpose of furthering knowledge and advising the federal government. Functioning in accordance with general policies determined by the Academy, the Council has become the principal operating agency of both the National Academy of Sciences and the National Academy of Engineering in providing services to the government, the public, and the scientific and engineering communities. The Council is administered jointly by both Academies and the Institute of Medicine. Dr. Frank Press and Dr. Robert M. White are chairman and vice chairman, respectively, of the National Research Council.

Transportation Research Board
National Research Council
2101 Constitution Avenue, N.W.
Washington, D.C. 20418

ADDRESS CORRECTION REQUESTED

NON-PROFIT ORG.
U.S. POSTAGE
PAID
WASHINGTON, D.C.
PERMIT NO. 8970

000021-05
Robert M Smith
Research & Asst Matls Supvr
Idaho Transportation Dept
P O Box 7129
Boise ID 83707-1129